



NTNU – Trondheim
Norwegian University of
Science and Technology

The Importance of Low-end-rheology and its Influence on Particle Slip Velocity

Elvin Guliyev

Petroleum Engineering

Submission date: October 2013

Supervisor: Pål Skalle, IPT

Co-supervisor: Aminul Islam, Statoil ASA

Norwegian University of Science and Technology

Department of Petroleum Engineering and Applied Geophysics

Acknowledgement

In the name of Allah, Most Gracious, Most Merciful

I would like to express my sincere thanks to the Norwegian University of Science and Technology for providing the opportunity to pursue my master degree in this university and ensuring all necessary facilities as well as to express my gratitude to all who are part of Norwegian University of Science and Technology for their support during the learning process and preparation of this master thesis.

I would like to acknowledge all the effort of all the people who have invested their time to my work and help me reach my goal. I would like to express my deepest gratitude to my supervisor Pål Skalle, who is embodiment of a such kind of professor who provides excellent suggestions and timely support, inspires and mentally stimulates his students to make constant progress in their researches and. I am glad to be among of his students. I would like also to thank him for his advices throughout the process of thesis writing.

I am very grateful to Roger Overå for his valuable advices during taking experiments in the laboratory. I would like to thank him for the discussions, which made great influence on my thesis.

Having this opportunity, I would like to express my sincere gratitude to all faculty members of the Department of Petroleum Engineering & Applied Geophysics for their kind cooperation and assistance during the whole period of my study at Norwegian University of Science and Technology.

Finally, I would like to express my gratitude to my family for their support and love throughout entire process by keeping me harmonious and confident. I would also like to thank all my friends who always stood by me. The completion of this thesis work was not possible without the help and guidance of all of them.

Above all, I would like to thank *Almighty Allah* upon successful completion of my master thesis.

All praise belongs to Almighty Allah Who created the world

Elvin Guliyev

Abstract

The study of effective cuttings transports and understanding fluid rheological properties is a major concern in the drilling industry. Poor hole cleaning can lead to cuttings accumulations inside the annulus, low rate of penetration (ROP), eccentric borehole, fluid loss and stuck pipe. However, introduction of low-shear-rate viscosity (low-end-rheology) mud system into drilling activities can significantly reduce aforementioned problems.

In this study, both theoretical analysis and experimental investigation were performed to estimate effects of low-end-rheology mud on particle settling velocity in a vertical cylinder, for static condition and steady state laminar flow in vertical annulus. Experimental tests were carried out in a flow-loop, using a low-end-rheology and standard rheology (water). Variables evaluated were particle size (0.3 mm, 1 mm, 2 mm), tube inner diameter or annular size (39.58 mm, 49.37 mm, 60.2 mm, 75 mm), fluid rheological parameters (water, mixtures of 5, 10 and 20 gram of PHPA Polymer per liter water), fluid condition (static and dynamic flow), particle sphericity (0.91 and 1). Fluid rheological parameters, particle size, and annular flow velocity were the most important variables. Annular flow velocities were 0 m/s for static and 0.00001-0.004 m/s for dynamic flow conditions. The experimental data showed that particles dropped in low-end-rheology fluid had a lower slip velocity compared to standard rheology.

Study of the rheology and factors influencing its properties were also part of this thesis work. During the tests, a fluid sample of 10% PHPA polymer-water mixture showed unexpected behavior. A detailed laboratory study verified that the rheological properties may change under the influence of mixing and no-action times and they are sensitive to the fluid shaking (shearing/stirring).

A comparison of the experimental particle settling velocities with particle settling velocities calculated by applying Stokes Law equation are also presented. Their results agree closely with experimental data for the slip velocity for particle settling in static and at steady state laminar flow for vertical annulus for the most of the cases. In other words, predicting of slip velocity by applying Stokes Law equation based on effective viscosity determined through Power Law fluid model showed favorable results for both quiescent and flowing fluid.

Sensitivity analysis based on the results concluded that particle transport in low-shear-rate-viscosity mud system provides better hole cleaning since the slip velocities of particles are lower compared to the standard rheology for the given experiment.

Table of Contents

Acknowledgement	I
Abstract.....	III
Table of Contents.....	V
List of Figures.....	VIII
List of Tables	X
1. Introduction.....	2
1.1 Goal	3
1.2 Approach.....	3
2. Review of the existening knowledge on slip velocity of sphere and cuttings.	5
2.1 Slip velocity	5
2.2 Rheology description.	7
2.2.1 Basic understanding of rheology	7
2.2.2 General.....	9
2.2.3 Fluid rheology models.....	11
2.3 Influence of rheology on particle settling.....	12
2.3.1 Shear rate of slipping particle in stagnant fluid.....	12
2.3.2 Shear rate of slipping particle in dynamic fluid.	13
2.3.3 Wall effects on a sphere motion in a fluid.....	14
2.4 Low shear rate viscosity.....	15
2.4.1 Background	15
2.4.2 Practical use of low-shear-rate-viscosity in oil-field industry	15
2.5 Model description.....	16
2.5.1 Stoke's law	16
2.7 Slip velocity correlation.....	18
2.7.1 Moore velocity correlation.	18
2.7.2 Chien velocity correlation	19
2.7.3 Mayes and Walker velocity correlation	19
3. Experimental study.	21
3.1 Test matrix.	21
3.2 Preparation for slip velocity test.....	22

3.3 Test equipment and instruments.....	23
3.4 Test procedure of slip velocity	26
4. Fluid results (or input data) ahead of the slip velocity test	28
4.1 Fluid rheological properties.....	28
4.2 Gel strength.....	29
4.3 Polymer solubility in a water medium.....	30
4.4 Time-dependency	31
4.5 Stirring of fluid just before a new test.....	32
5. Test results of slip velocity	34
5.1 Slip velocities of static condition.....	34
5.1.1 Experimental results	34
5.1.2 Theoretical results.....	38
5.1.3 Comparison	41
5.2 Slip velocities of dynamic condition.....	42
5.2.1 Flow dependence	42
5.3 Comparison	43
6. Discussion	45
6.1 Discussion of Fluid tests.....	45
6.2 Discussion of Experimental set-up.....	46
6.3 Discussion of the error related to the experimental results.....	47
7. Conclusion	49
8. Recommendation	50
Abbreviation	51
Nomenclature.....	52
References.....	54
Appendix A. Experimental device and particles.....	56
Appendix B. Rheological properties of all three fluids samples used during measuring of slip velocities	58
Appendix C. Calculated (theoretical) results of stagnant condition	59
Appendix D. Calculated (theoretical) results of dynamic condition.....	61
Appendix E. Experimental results of slip velocities in a stagnant fluid	62
Appendix F. Rheological properties of sample 10% used for the detection of root causes of unexpected behavior (mixing time/ solubility of polymer).....	64

Appendix G. Rheological properties of sample 10% used for the detection of root cause of unexpected behavior (no action time/ waiting time).....	65
Appendix H. Rheological properties of sample 10% used for the detection of root cause of unexpected behavior (shaking factor).....	66
Appendix I. Drag coefficient and particle Reynolds number exported from the figure 8.....	67
Appendix J. Simple calculation used during experimental investigation	68

List of Figures

<i>Figure 1. Vertical forces acting on single sphere (University of Tennessee 2008).</i>	5
<i>Figure 2. Shear stress and shear rate (Ford 2003).</i>	8
<i>Figure 3. Variation of effective viscosity slope with increasing of shear rate based on reading from Fann 35 viscometer of 10-gram PHPA Polymer per liter water (Table B-1).</i>	10
<i>Figure 4 . Fluid stress and velocity distribution in circular pipe (COSMOS 2008).</i>	11
<i>Figure 5. Particle settling and shear rate around it in stagnant fluid.</i>	13
<i>Figure 6. Drag coefficient (Friction factor) versus Reynolds number chart used for calculating of particle slip velocity based on particles different sphericities (A.T. Bourgoyne Jr, K.K. Millheim et al. 1986).</i>	18
<i>Figure 7. Schematic drawing of apparatus used for measure of cuttings slip velocity in quiescent and at steady state laminar fluid flow (low shear rate).</i>	24
<i>Figure 8. Fann 35 viscometer(Anon 2013).</i>	25
<i>Figure 9. a) Mud balance (left)(Anony. 2013) and b) Waring laboratory blender(right)(Anon 2013)</i>	26
<i>Figure 10. Viscosity curves for all three fluid samples measured with Fann 35 viscometer at ambient temperature and compared with theoretical curves for samples 5% and 10% (based on two upper data points) and for sample 20% (based on four upper data points) are drawn black.</i>	29
<i>Figure 11. Ten seconds, one minute and ten minutes gel strength measurements for all three fluid samples at ambient temperature.</i>	30
<i>Figure 12. Trend of viscosity curves of four different fluid with 10 gram of PHPA polymer concentration 10 gram per liter of water each with respect to mixing time</i>	31
<i>Figure 13. Increase in rheological properties of fluid sample 10% with no-action time (measured immediately, after one and three days)</i>	32
<i>Figure 14. Variation in viscosity properties of fluid sample 10% with respect to the shaking (stirring) time.</i>	33
<i>Figure 15. Effect of cylinder wall and annular space on slip velocity of 1 mm spherical particle conducted in fluid sample 5% (Table E-2).</i>	35
<i>Figure 16. Effects of all three fluid samples rheological properties and particle size on particle slip velocities.</i>	37
<i>Figure 17. Change in particle slip velocities of 1mm and 2 mm particles size in fluid sample 5% with respect to travel length.</i>	38
<i>Figure 18. Experimental correlation of the drag coefficient with the particle Reynolds number for all three fluid samples in laminar flow compared with the published drag coefficient versus particle Reynolds number</i>	39

Figure 19. The correlation of slip velocities with particles Reynolds number for all three fluids samples	40
Figure 20. Correlation of particle Reynolds number with particle size in all three fluids samples	41
Figure 21. Comparison between observed and calculated slip velocity for all particle size in all three fluid samples.....	42
Figure 22. Comparison of the slip velocity results in stationary and dynamic fluid conducted in mixture of 5 gram PHPA polymer per liter water	43
Figure 23. Comparison of theoretically proposed shear rates around particle with experimental results in fluid sample 5%.	44
Figure 24. Experimental device used for investigation of particle slip velocity under steady state laminar flow	56
Figure 25. Non-spherical particle used during experimental investigation (d=3.387mm).....	56
Figure 26. Spherical particle used during experimental investigation (d=2mm).....	57
Figure 27. Non-spherical particle used during experimental investigation (d=3.387mm).....	57

List of Tables

Table 1. Test matrix	21
Table 2. Rheological properties of 5% PHPA polymer-water mixture.	58
Table 3. Rheological properties of 10% PHPA polymer-water mixture	58
Table 4. Rheological properties of 20% PHPA polymer-water mixture	58
Table 5. Experimental data (and input data (blue) and theoretically calculated results (red) based on shear rates of v/d for fluid sample 5%	59
Table 6. Experimental data (and input data (blue) and theoretically calculated results (red) based on shear rates of $3*v/d$ for fluid sample 5%	59
Table 7. Experimental data (and input data (blue) and theoretically calculated results (red) based on shear rates of v/d for fluid sample 10%	59
Table 8. Experimental data (and input data (blue) and theoretically calculated results (red) based on shear rates of v/d for fluid sample 20%	60
Table 9. Input data (blue) and theoretically computed result for steady state laminar flow in sample 5%	61
Table 10. Input data (blue) and theoretically computed results for steady state laminar flow in sample 5%	61
Table 11. Experimental results of slip velocities with respect to particle sizes and tube diameters conducted in standard rheology (water).....	62
Table 12. Experimental results of slip velocities with respect to particle size and tube diameters conducted in sample 5%	62
Table 13. Experimental results of slip velocities with respect to particle size and tube diameters conducted in sample 10%	62
Table 14. Experimental results of slip velocities with respect to particle size and tube diameters conducted in sample 20%	62
Table 15. Experimental results of 1mm particle slip velocities with respect to the travel distance in fluid sample 5%	63
Table 16. Experimental results of 2 mm particle slip velocities with respect to the travel distance in fluid sample 5%	63
Table 17. Rheological properties of the sample 10% measured after 40 seconds of mixing ..	64
Table 18. Rheological properties of the sample 10% measured after 65 seconds of mixing ..	64
Table 19. Rheological properties of the sample 10% measured after 150 seconds of mixing	64
Table 20. Rheological properties of the sample 10% measured after 170 seconds of mixing	64
Table 21. Rheological properties of the sample 10% measured immediately right after the mixing in blender.....	65

Table 22. Rheological properties of the sample 10% measured after one day since mixed in blender	65
Table 23. Rheological properties of the sample 10% measured after three days since mixed in blender	65
Table 24. Rheological properties of 10% PHPA polymer-water mixture after 15 seconds of shaking.....	66
Table 25. Rheological properties of 10% PHPA polymer-water mixture after 30 seconds of 66	
Table 26. Rheological properties of 10% PHPA polymer-water mixture after 60 seconds of shaking.....	66
Table 27. Data acquired from Applied Drilling Engineering(A.T. Bourgoyne Jr, K.K. Millheim et al. 1986) presented in figure 8 that shows correlation between Drag coefficient (friction factor) and particle Reynolds number.	67

1. Introduction

Transport of cuttings from the bottom hole up to the surface through the annulus is one of the primary objectives of a drilling mud. Failure to accomplish this function will lead to cuttings accumulation in the lower part of the annulus. In fact, poor hole cleaning and inefficient cuttings transport may lead not only to the cuttings accumulation but also to several unwanted problems such as excessive equivalent circulating density (ECD), high torque and drag, lost circulation, formation fracture and stuck pipe during drilling operation. All that events increase the non-productive time (NPT) and costs (Pilehvari, Azar et al. 1999). The most severe cuttings accumulation takes place in highly deviated wellbore, where cuttings fall to the lower side of annulus due to gravity force. This process causes cuttings agglomeration at more sustainable part of the annulus, e.g. horizontal section of the annulus.

The major factors that describe cuttings transport are fluid velocity and particle settling velocity. For efficient cleaning of the wellbore, fluid velocity must prevail cuttings settling velocity and has to be sufficient to transport these cuttings to the surface. The least velocity that is required to transport cuttings is defined as minimum annular fluid velocity (Larsen, Pilehvari et al. 1997). Slip velocity (or settling velocity) is a velocity at which settling of drilled solids occurs relative to the annular fluid velocity. In general, settling of particles occurs due to gravity. The slip velocity of particles depends also on sphericity, size of the drilled cuttings and under the influence of rheology valid for cuttings movement (HOPKIN 1967).

In stagnant mud, the cuttings are suspended and do not settle under gravity influence, since gel strength and yield stress contribute to the suspension of the particles in a fluid medium. During circulation, mud starts to shear and the yield stress at one point will be overreached. This phenomenon leads to settling of cuttings under gravity force. A best practice is to apply Stokes law into this system. Stokes law says, that the cuttings fall down under gravity and lift due to buoyancy and drag force. Hence, if the gravity force overcomes the drag and buoyancy forces, it will result in particle settling and the cuttings will start to fall down (Alcocer, Ghalambor et al. 1992).

The main scope of this study is to investigate cuttings slip velocity in stagnant (still-stand) fluid and at laminar fluid flow. Low-end-rheology is the rheology of the mud that is observed at low fluid shear rates. This means, that the low-end-rheology of the mud is high when the

shear rate is so low (Herzhaft, Rousseau et al. 2002). The purpose of designing of low-end-rheology is to provide efficient cuttings transport and hole cleaning. The low-end-rheology will result in a better carrying capacity of a drilling mud; it will provide suspension of barite and drilled cuttings. Thereby, to define the importance of properties of low-end-rheology we have to compare it, when we estimate slip velocity of the fluid under static conditions and dynamic flow (or at low shear rate) with normal rheological parameters of Newtonian fluid (or at high shear rate of viscous fluid). Before proceeding to the experimental part, it would be useful to describe the process theoretically.

One important issue to describe/investigate is the rheological behavior of the fluid during flowing condition. Since, fluid during laminar flow experiences low shear rate, the cutting movement in fluid will increase shearing of layers around the particle. Thus, fluid will shear more, and (theoretically) it will result in relatively faster settling.

The particle settling velocity is also affected by particle shape, which is determined by the sphericity factor ϕ . Since, the drag coefficient increases with decreasing sphericity, the settling of cuttings particle is occurring faster for sphere rather than non-spherical particle (A.T. Bourgoyne Jr, K.K. Millheim et al. 1986).

Finally, it is worth mentioning, that there has previously been little investigation on low-end-rheology.

1.1 Goal

The main goal of this study is to determine the influence and the importance of applying low-end-rheology on cuttings slip velocity for a drilling fluid at rest and at steady state laminar flow and standard rheology (water) at quiescent condition and compare theoretical results with measured results of slip velocity by means of the Stokes Law equation.

1.2 Approach

To match the goal we need to consider following steps:

- The first step is to conduct a literature review that introduce the low-end-rheology and all aspects of the experiment and all possible solutions of this issue.

- The second step is to plan an experimental investigation and construct it in order to conduct experimental test to evaluate slip velocity in vertical wells during static and laminar flow (at low shear rate).
- Apply the standard Fann 35 viscometer and mud balance to evaluate all required rheological properties of fluids.
- The fourth step of study is theoretically describe slip velocity model for vertical based on Stoke's Law during stagnant and laminar flow and compare the results by applying two different theological approaches.
- The final step is to compare measured and estimated results to define the importance of low-end theology on cuttings transport.

2. Review of the existening knowledge on slip velocity of sphere and cuttings.

2.1 Slip velocity

During drilling operations, a fluid pumped into the wellbore in order to circulate the cuttings out of the well. Soon, as fluid pumped in, it reaches its determined annular transport velocity. Flowing fluid exerts hydrodynamic drag force on a particle and retards particle settling which in turn affects on particle slip velocity. Failure of mud to accomplish its function leads to severe settling of cuttings. This results in cuttings accumulation at bottom or at lower side of the wellbore depending on well inclination.

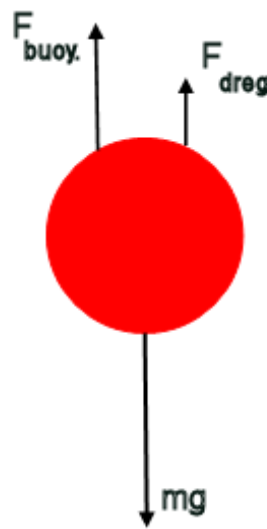


Figure 1. Vertical forces acting on single sphere (University of Tennessee 2008).

A solid particle inside the fluid that is allowed to settle will be falling at a constant velocity, which shall be referred to as a terminal settling velocity (or a constant slip velocity) (Sifferman, Myers et al. 1974). However, it has to be noted, that due to the differences between the particles, the slip velocity of any particle is different. The differences are determined by several factors such as fluid and cuttings properties (HOPKIN 1967).

As soon as a particle starts to travel in a viscous fluid, it attains a constant velocity. This happens because of dynamic equilibrium of the net forces, which are vertical and acts upon the particle as it is described in **figure 1**. The forces mentioned should be considered (Machado and Aragao 1990).

- the upward force due to resistance of fluid (viscous drag) around the particle
- the upward force due to buoyancy
- the downward force due to gravity

As it is stated above, the factors influencing particle slip velocity is a particle diameter, shape and specific gravity. The viscosity properties and density of a fluid also affect settling rate. In addition, (Krumbein 1939) mentioned in his paper the importance of the particle orientation on particle settling velocity and cuttings transport.

For flatwise particles, two types of settling pattern (orientation) were observed: stable settling and oscillation (swinging) settling. Due to flatwise body, a disk tends to settle with its largest surface area faced to the bottom. This type of orientation is called stable settling. In case of oscillation settling, a disk fall reminds swinging, where the orientation and ring stabilities are lost together (Fang 1992).

2.2 Rheology description.

Fluid rheological properties (viscosity parameters and density) play an important role on effective cuttings transport. For instance, high viscosity of mud provides resistance to the particle, so the particle settling occurs very slowly. For some of the fluids, viscosity decreases with flow of the fluid. This means, fluid movement creates shearing of the fluid layers, which in turn decreases viscosity of the mud. In addition, particle settling also provides additional shear, which negatively affects slip velocity.

2.2.1 Basic understanding of rheology

Rheology is defined as a study of the flow and deformation of the matter (Mezger 2011). The study of the rheology is essential, because it allows us to design our drilling fluid in order to get efficient hole cleaning, to minimize pump pressure, to prevent loss of circulation into drilled formations, etc. Apart from it, rheological properties can influence barite suspension and solids control.

Viscosity

Resistance of a fluid to flow is defined as viscosity. Basic concept of the viscosity can be described in terms of shear stress (τ) and shear rate (γ).

Shear Stress

To understand the concept of the viscosity, consider fluid between two layers with constant area A (**Figure 2**). The lower plate is remaining in a static condition, however the upper layer will start to move after force F is applied. The movement of the layer of a given area A induced by force F is called shear stress. It can be expressed as (Hughes 2006):

$$\tau = \frac{F}{A} \quad (1)$$

Shear Rate: Applying the force F will result in a shear movement of the upper layer relative to the lower layer at a velocity v (**Figure 2**). The movement rate of the fluid between layers is defined as shear rate. Since the flow velocity of any fluid is the highest at the center of the pipe, the shear rate will be zero; conversely, at the pipe wall, the flow velocity reaches its minimum and the shear rate its maximum (Hughes 2006).

The shear rate can be defined by the following equation:

$$\gamma = \frac{v_2 - v_1}{d} \quad (2)$$

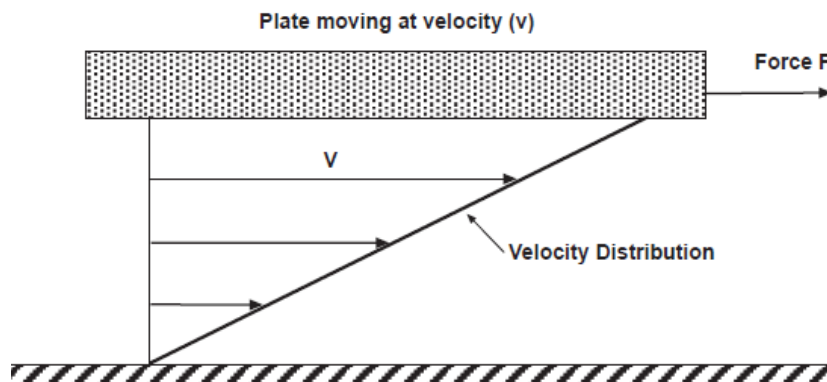


Figure 2. Shear stress and shear rate (Ford 2003).

Yield Point (YP): Resistance to flow induced by electrochemical forces between any particle in fluid is called yield point (or yield stress). This force is the result of attraction between positively charged sites on edge of clay layers with negatively charged on surface of clay layers (Hughes 2006).

- volume concentration of solids in fluid system
- the surface properties of the mud solids
- electrically charged environment of solids

Calculation of yield point value based on readings from Fann 35 viscometer is as follows:

$$\text{Yield Point} = \tau_o = \theta_{300} - \mu_{pl} \quad (3)$$

Gel strength: The gel strength of a drilling mud defines its ability to suspend cuttings and weighting materials when circulation stops. Usually, its measurements show the time-dependent flow behavior of the liquid, which are measured at 10 seconds, 1 minute, and 10 minutes time span.

Gelling is caused by the presence of electrically charged particles (molecules) or by ability of polymers link with each other. Particle (polymer) concentration, chemical treatment, temperature and time can severely affect on gelling properties (Hughes 2006).

2.2.2 General

Newtonian Fluid

For Newtonian fluid, viscosity of mud is expressed by the relationship between shear stress and shear rate. Viscosity of mud remains constant at all shear rates and provides constant value at all rates. It can be expressed by the following equation:

$$\mu = \frac{\tau}{\dot{\gamma}} \quad (4)$$

Non-Newtonian Fluid.

Unlike the Newtonian fluid, viscosity of non-Newtonian fluid does not have constant viscosity that can describe fluid behavior at all shear rates. Therefore, in order to evaluate viscosity of non-Newtonian fluid at a specific shear rate, the expression "effective viscosity" (apparent viscosity) is introduced. Effective viscosity is the term used to describe the viscosity of non-Newtonian fluid at a particular shear rate (**Figure 3**). The term itself takes into consideration the geometry of the medium through which the fluid is flowing, e.g. pipe.

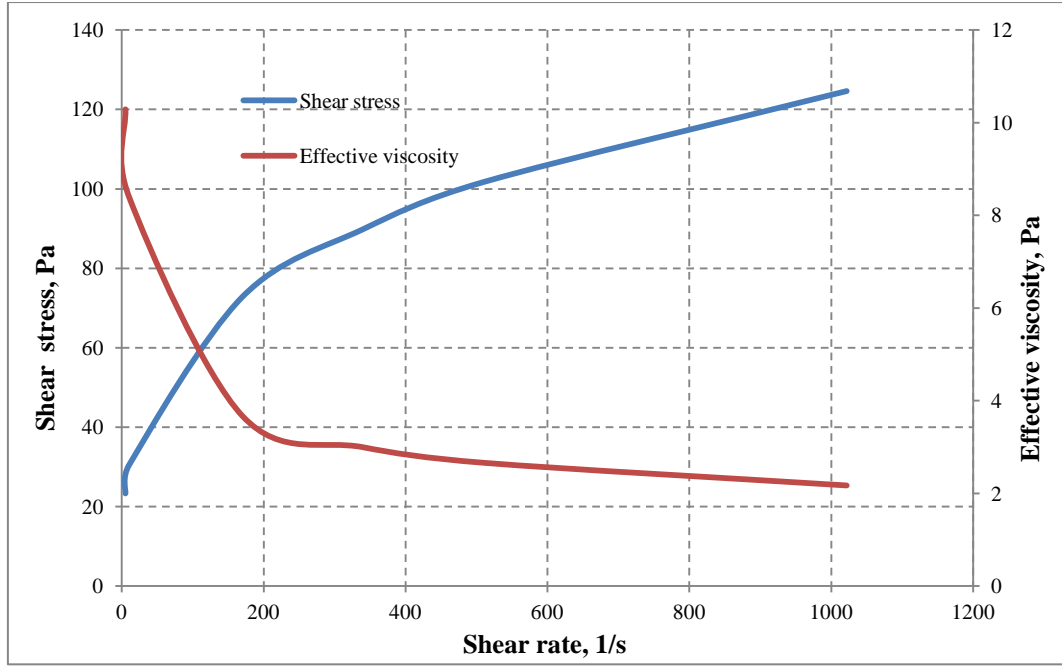


Figure 3. Variation of effective viscosity slope with increasing of shear rate based on reading from Fann 35 viscometer of 10-gram PHPA Polymer per liter water (Table B-1).

Fluid flowing through pipe experiences retarding (friction) force between the layers. Due to no slip between fluid layer and pipe wall, fluid requires high shear stress at the flow boundary (pipe wall). Hence, flow is easier in the middle of the pipe rather than at pipe wall. Thereby, fluid tends to stretch out in center of pipe (high velocity) and retards at the pipe wall (**Figure 4**).

Therefore, shear rate at pipe wall will be at maximum and it can be expressed as :

$$\gamma_w = \frac{8v}{d_{dp}} \quad (5)$$

By applying the Newtonian effective viscosity model (equation 1) and shear rate (equation 2) for Power Law Fluid model, the effective viscosity for shear-dependent fluid becomes:

$$\mu_{eff} = \left(\frac{8v}{d_{dp}} \cdot \frac{3n+1}{4n} \right)^n \frac{Kd}{8v} \quad (6)$$

The Power Law fluid will be explained in the following section.

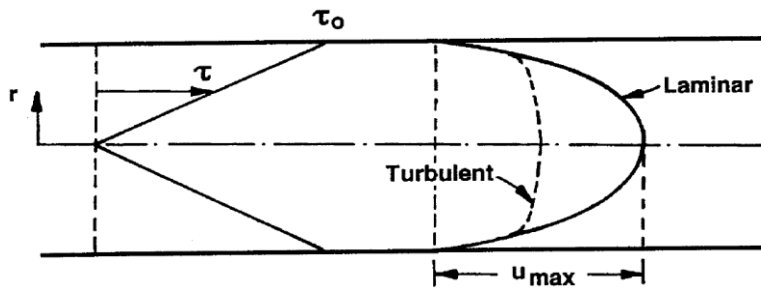


Figure 4 . Fluid stress and velocity distribution in circular pipe (COSMOS 2008).

2.2.3 Fluid rheology models

Power-Law Model

Power-Law fluid model gives a good behavioral description of the shear-thinning and shear-thickening fluids. It precisely describes fluid behavior at very low shear rates. However, it is ineffective at very low shear stress, since Power-Law model does not include the yield stress.

Power law fluid model can be expressed by

$$\tau = K * \gamma^n \quad (7)$$

The term K is defined as consistency factor and describes the thickness of drilling fluid. The exponent n is called the flow behavior index and can be expressed as (A.T. Bourgoyne Jr, K.K. Millheim et al. 1986):

$$n = \frac{\log \tau_1 / \log \tau_2}{\log \gamma_1 / \log \gamma_2} \quad (8)$$

Flow behavior index indicates the degree of Non-Newtonian behavior. For

- $n > 1$, the fluid shows shear-thickening properties and defined as a dilatant
- $n=1$, the fluid shows Newtonian behavior
- $n < 1$, the fluid shows shear-thinning properties and defined as a pseudoplastic fluid

Herschel-Bulkley Model

Herschel-Bulkley model is a unique mathematical model for describing fluid behavior. Actually, this model can describe the approximate behavior of drilling fluid and gives accurate results at very low shear stress (Hughes 2006).

The model is expressed below:

$$\tau = \tau_o + K * \gamma^n \quad (9)$$

The constants K and n describe the same functions as in Power-law model and τ_o is a yield point.

2.3 Influence of rheology on particle settling

2.3.1 Shear rate of slipping particle in stagnant fluid.

For non-Newtonian fluid, the effective viscosity primarily depends on the shear rates. In case, if settling happens in a stagnant non-Newtonian mud, the shear rate on a particle equals to the particle slip velocity divided by its diameter (v/d). Since particle settling is the only source of fluid shearing, the effective viscosity for Power Law Fluid model becomes (Novotny 1977):

$$\mu_{eff} = K \left(\frac{v_s}{d_p} \right)^{n-1} \quad (10)$$

(Daneshy 1978) proposed to use $\left(3 \frac{v_p}{d_p} \right)$ instead of mentioned $\left(\frac{v_p}{d_p} \right)$ to describe shear rate caused by particle settling in quiescent fluid. Effective viscosity for Power Law Fluid model can be described by:

$$\mu_{eff} = K \left(3 \frac{v_s}{d_p} \right)^{n-1} \quad (11)$$

Figure 4 illustrates the particle settling in stagnant fluid and the shear rate around the particles.

2.3.2 Shear rate of slipping particle in dynamic fluid.

A further complication shows up for flowing non-Newtonian fluids, since the shear rate imposed on a particle in the direction of fluid movement, as well as the shear rate because of the particle slipping. In order to define the significance of this effect, several experiments with single proppant particle in concentric cylinders were proposed by (Novotny 1977).

According to the experimental results, for the case, when a Newtonian fluid was used, the shear rate imposed on a particle did not affect the slip velocity of proppant particle. Such results were expected, since viscosity of Newtonian fluid does not vary with a shear rate. However, when a non-Newtonian fluid was used, particle settling occurred faster during shearing compared to the static condition (**Figure 5**) (Novotny 1977).

Thereby, the total shear rate γ_t on a proppant particle was determined to be the vector sum of the shear rates due to particle sinking $(\frac{v_s}{d_p})$ and the shear rate γ_f imposed by fluid movement.

$$\gamma_t = \sqrt{\left(\frac{v_s}{d_p}\right)^2 + \gamma_f^2} \quad (12)$$

Effective viscosity for Power Law fluid around the spherical particle during flowing of fluid can be expressed by the following equation:

$$\mu_{eff} = K \left[\left(\frac{v_s}{d_p}\right)^2 + \gamma_f^2 \right]^{\frac{1-n}{2}} \quad (13)$$

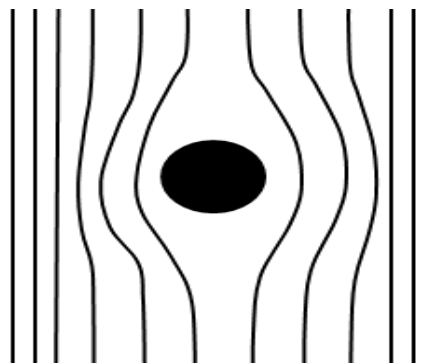


Figure 5. Particle settling and shear rate around it in stagnant fluid

2.3.3 Wall effects on a sphere motion in a fluid.

The slip velocity of particle in a stagnant fluid is considerably reduced by the existence of the cylinder wall. The hindrance effect of the cylinder wall on sphere motion in fluid is defined as a wall effect. This effect is induced by the upward movement of the fluid and it depends on the space between cylinder wall and the particle.

The wall effect has been quantified in terms of the wall factor f . The wall factor f is determined as the ratio of the slip velocity of particle in confined medium to the slip velocity of the same particle in infinite medium.

$$f = \frac{V_{s,f}}{V_{s,\infty}} \quad (14)$$

The severity of this factor is influenced by the particle-to-tube diameter ratio ($\lambda = d_p / D$) and particle Reynolds number. In fact, it has been agreed that wall factor is independent of particle Reynolds number at very low Reynolds number region and at very high Reynolds number region, but being dependent at transitional regime. It is estimated, that the wall factor f is a function of particle-to-tube diameter at very low and at very high values of the particle Reynolds number by following equations (Di Felice, Gibilaro et al. 1995):

laminar flow

$$f = \frac{1 - 2.105\lambda + 2.0865\lambda^3 - 1.7068\lambda^5 + 0.72603\lambda^6}{1 - 0.75857\lambda^5} \quad \lambda \leq 0.9 \quad (15)$$

turbulent flow

$$f = (1 - \lambda^2)(1 - 0.5\lambda^2)^{0.5} \quad 0 \leq \lambda \leq 1 \quad (16)$$

(Liu and Sharma 2005) referring to their experimental work concluded that in Power Law fluid, increase in effective viscosity (apparent) of the fluid for a single particle reduces the retardation effect of the wall.

2.4 Low shear rate viscosity.

2.4.1 Background

Low-shear-rate-viscosity is an almost-zero constant shear rate measurement taken in the span of 0.06 1/sec. It measures both components of viscosity: viscous and elastic. Under flowing condition, in horizontal and highly deviated wellbores, low-shear-rate-viscosity correlates to modified fluid properties, which enhance transport and provide suspension of cuttings, reduce radial slip velocity of the drilled and suspended cuttings and partly eliminate cuttings agglomeration in lower part of the wellbore. Under static condition, in horizontal and highly deviated wellbores, low-shear-rate-rheology correlates to suspension of particles, minimizes radial slip of cuttings and decrease any likelihood for the accumulation of cuttings beds (Powell, Parks et al. 1991).

2.4.2 Practical use of low-shear-rate-viscosity in oil-field industry

Nakajima and Bot (2002) together with Japan Vietnam Petroleum Company introduced enhanced low-shear-mud-viscosity mud system into the highly deviated and horizontally extended well, where the hole cleaning and agglomeration of cuttings in the wellbore became a serious issue (Nakajima and Bot 2002).

As they had supposed, the low-shear-rate-viscosity improved the efficiency of the hole cleaning by strengthened rheological mechanism and also resulted in increase of average penetration rate (ROP). The main function of this mud system was to improve efficiency of hole cleaning by a strengthened rheological mechanism (Nakajima and Bot 2002).

There are not that much studies and experiments with low-shear-rate-viscosity, which restricts gaining knowledge and giving detailed explanation on importance of low-end-rheology. However, there will be conducted experiments with low-shear-rate-viscosity mud system in order to define their significance in industry. In the following chapter there will be some recommendations about usefulness of the aforementioned mud system.

2.5 Model description

2.5.1 Stoke's law

The model introduced in this study aims to explain the basic principle of the Stokes Law. There are several assumptions, which listed further in this sub-chapter.

Stokes's law can be described as a phenomenon, in which a spherical particle of a known density and size tends to settle through a stagnant fluid of infinite extent. The particle attains its constant settling velocity, as soon as it starts to move. Knowing the rheological properties, the density and size of the particle, Stoke's law can be used to calculate the slip velocity of the particle. The following assumptions should be taken into consideration during derivation of slip velocity by applying Stoke's Law (Alcocer, Ghalambor et al. 1992).

- Particle settles through a stagnant or laminar flowing fluid
- Vertical (gravity, buoyancy and drag) forces are in equilibrium.
- Fluid compared to the size of the cuttings should be homogeneous
- No slippage between particle and fluid.
- Particle movement should be independent
- Terminal settling velocity should be reached very soon
- Particle must settle as it would in unbounded medium

As it was mentioned in chapter 2.1, as soon as particle starts to travel in viscous fluid, it attains its constant velocity, so that the sum of the forces acting on a particle are equal to zero. This means that the sum of the forces acting in upwards direction due to buoyancy F_b and resistance F_d of the fluid is precisely counterbalanced by the gravity force F_g (A.T. Bourgoyne Jr, K.K. Millheim et al. 1986).

The general equation of the sum of the vertical forces is expressed by

$$F_g - F_b = F_d \quad (17)$$

By defining all the forces, the aforementioned equation is solved:

$$(\rho_p - \rho_f)g\left(\pi \frac{d_p^3}{6}\right) = 3\pi d_p \mu v_s \quad (18)$$

Rearranging the equation yields the following relationship:

$$v_s = \frac{d_p^2 \cdot g \cdot (\rho_p - \rho_f)}{18\mu} \quad (19)$$

Stoke's law is can be used to determine sphere slip velocity in Newtonian fluids as long as laminar flow presents around the particle. Applicability of **equation 3** depends on the sphere Reynolds number, which is a function of fluid rheological properties, particle size and slip velocity:

$$N_{RE} = \frac{\rho_f d_p v_s}{\mu_{eff}} \quad (20)$$

Reynolds number below 0.1 gives accurate value of slip velocity. However, for Reynolds number above 0.1, the empirical drag coefficient C_{drag} (or friction factor F_f) must be introduced (A.T. Bourgoyne Jr, K.K. Millheim et al. 1986). (Applied Drilling Engineering)

$$C_{drag} = \frac{4d_p g (\rho_p - \rho_f)}{3v_s^2 \rho_f} \quad (21)$$

However, cuttings are not always truly spherical. Most of them have a non-spherical shape. Since, shape of particles are different, the sphericity factor ψ has to be used. Ratio of the surface area of a spherical particle having the exact volume as the particle divided by the surface area of the non-spherical particle is defined as sphericity .

Sphericity is defined as the ratio of the surface area of a sphere containing the same particle volume as the particle divided by the surface area of the particle (copied) (Applied drilling engineering)

Figure 6 demonstrate correlation of drag coefficient (friction factor) with particle Reynolds number for estimating particles slip velocities with respect to the their sphericities.

The drag coefficient equation can be rearranged for the estimation of particle settling velocity that expressed by:

$$v_s = \sqrt{\frac{4gd_p}{3C_{drag}} \left(\frac{\rho_p - \rho_f}{\rho_f} \right)} \quad (22)$$

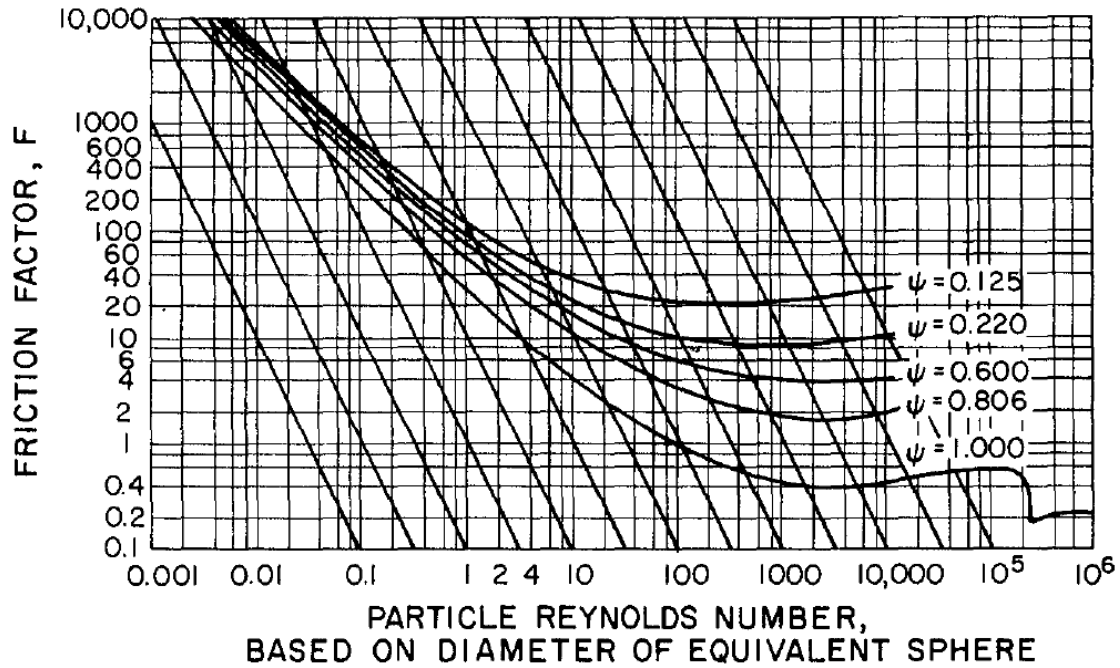


Figure 6. Drag coefficient (Friction factor) versus Reynolds number chart used for calculating of particle slip velocity based on particles different sphericities (A.T. Bourgoyne Jr, K.K. Millheim et al. 1986).

2.7 Slip velocity correlation

2.7.1 Moore velocity correlation.

Preston Moore suggested a technique for calculating particle slip velocity that takes into consideration non-Newtonian behavior of the drilling mud and utilizes equations of the drag coefficient and sphere Reynolds number relation for particle settling through a Newtonian fluid. The suggestion was to use an effective (apparent) Newtonian viscosity that was first proposed by Metzner and Dodge in 50ies of the previous century. It simply obtained by equating annular friction pressure losses expressions for Power Law Fluid model and for Newtonian model and solving for effective Newtonian viscosity. The effective Newtonian viscosity expression derived from the aforementioned technique is given as (in oil field unit) (Sample and Bourgoyne 1977).

$$\mu_{eff} = \frac{K}{144} \left(\frac{d_2 - d_1}{v_a / 60} \right)^{1-n} \left(\frac{2 + \frac{1}{n}}{0.0208} \right)^n \quad (23)$$

Then, the effective Newtonian viscosity was used to calculate the solid Reynolds number expressed by **equation 20**. For particle, Reynolds number below value 1, the flow regime

around the cutting is considered as laminar and the drag coefficient correlation can be calculated by:

$$C_{drag} = \frac{40}{N_{Re}}$$

(24)

Substituting the drag coefficient **equation 24** into the **equation 19** and converting into oil field units, yields the following equation for particle settling velocity

$$v_s = 4972 \frac{d_p^2}{\mu_a} (\rho_p - \rho_f) \quad (25)$$

2.7.2 Chien velocity correlation

The slip velocity correlation proposed by (Chien 1969) involves the computation of effective Newtonian viscosity for polymer-type drilling fluid.

$$\mu_a = \mu_{pl} + 5 \frac{\tau_y d_p}{v_a} \quad (26)$$

For bentonite-water mix system, it was definitely recommended to use a plastic viscosity as an effective (apparent) viscosity. The slip velocity correlation proposed for a lower particle Reynolds numbers becomes (A.T. Bourgoyne Jr, K.K. Millheim et al. 1986).

$$v_{slip} = 0.0075 \left(\frac{\mu_a}{\rho_f d_p} \right) \left[\sqrt{\frac{36800 d_p (\rho_p - \rho_f)}{\rho_f} + 1} - 1 \right] \quad (27)$$

2.7.3 Mayes and Walker velocity correlation

The technique suggested by (Walker and Mayes 1975) employs drag coefficient defined for a circular disk settling with their flat surface area faced downwards.

$$C_{drag} = \frac{2gh}{v_{slip}^2} \left(\frac{\rho_p - \rho_f}{\rho_f} \right) \quad (28)$$

For the computation of particle Reynolds number, an empirical relationship was developed for estimating the fluid shear stress induced by cuttings slippage, the following equation presented in oil field units(Sample and Bourgoyne 1977) :

$$\tau_f = 7.9\sqrt{h_s(\rho_p - \rho_f)} \quad (29)$$

Obtained shear stress τ value corresponds to the shear rate γ that was determined by using a plot of Fann dial reading versus shear rate (revolution multiplied by 1.703) obtained by using a Fann 35 viscometer. The effective viscosity used for estimation of the particle Reynolds number can be expressed by

$$\mu_{eff} = 479 \frac{\tau}{\gamma} \quad (30)$$

The slip velocity equation for particle Reynolds number below 100, the following equation is expressed in oil field units

$$v_s = 0.0203\tau \sqrt{\frac{d_p \gamma}{\rho_f}} \quad (31)$$

It has to be highlighted that this effective (apparent) viscosity is based on the relative shear rate of the particle experienced by the fluid and does not take into consideration, the shear rate provided by the fluid flow in annuli (A.T. Bourgoyne Jr, K.K. Millheim et al. 1986).

3. Experimental study.

The purpose of the current chapter is to present experimental work for determining the particle slip velocity when the fluid is still-standing and when it is flowing at a steady state laminar flow. The trial test will also help to compare the influence of shear rate due to flow on low-end-rheology. Obtained experimental results will be compared to theoretical slip velocity in order to evaluate the influence of the rheological model in predicting slip velocity.

This experimental study was conducted in a simple test facility (one-meter long vertical pipe). Details of the test facilities can be found below.

This experimental study was conducted in a simple test facility principally one meters long vertical pipe. Details of the test facilities are found below.

3.1 Test matrix.

Before measuring slip velocity of falling cuttings, one has to consider the variables of the experiment. The following test matrix was decided to be used in the research study for a better understanding of cuttings transport in the hole. Choice of the variables was based on previous investigation and self-analysis. The test matrix for the experimental investigation is presented in **table 1**. Demonstrated variables in mentioned table, simply shows how many types of each variable was used. For example: during the experiment five different ID cylinders were used, where four of them were used in static and one of them in dynamic test.

Table 1. Test matrix

Particle size	mm	0.3	1	2	3.387
Particle sphericity	-	1	1	1	0.91
Plane Water	-				
Polymer concentration	%	5%	10%	20%	
Travel Length	m	0.2	0.24	0.27	0.75
Pipe ID	mm	39.58	49.37	60.2	75 76.2
Fluid flow (quiescent)	m/s	Static	Steady state laminar		

Two types of tests were carried out during the experimental investigation. First type or base case was conducted for a static condition with respect rheology (standard and low-end), travel length, tube size and particle size (Figure A-2, A-3, A-4) separately. Second type or special

case was conducted in laminar flow conditions with respect to particle size at fluid polymer concentration of 5 gram per liter.

3.2 Preparation for slip velocity test.

a) **Density of particle.** Density of the solid particles was found by the ratio of the particles' mass to the volume increased in the graduated cylinder, which can be expressed as:

$$\rho_p = \frac{m_p}{V_p} \quad (32)$$

b) **Particle size.** To account for correct diameter of non-spherical particle, the equivalent spherical diameter (ESD) term were used. The diameter of particles was measured by Vernier caliper at different angles. Then, the sum of the measured diameter was divided by the number of measuring in order to find the average or ESD. The equation below describes mathematical way of defining the ESD:

$$d_{ESD} = \frac{d_1 + d_2 + d_3}{3} \quad (33)$$

c) **Particle sphere.** To calculate sphericity of a non-spherical particle, the surface area of a sphere having the same volume as the particle is divided by the surface area of the particle. This expression can be expressed as:

$$\psi = \frac{\pi^{\frac{1}{3}} (6V_p)^{\frac{2}{3}}}{A_p} \quad (34)$$

For the experimental purpose, the shape of the non-spherical particle assumed to be same as dodecahedron with sphericity equals to 0.91 (Wolfram Company 2013). Nevertheless, attempt to calculate the sphericity of the particle were done (the basic calculation were conducted to define sphericity of particle) and result demonstrated in **Appendix J**

d) **Fluid viscosifiers.** The main purpose of fluid rheology modeling was to design three drilling fluids with different viscosity properties in order to compare settling velocity of the particles. These fluid samples are categorized into three groups:

1. 5% PHPA Polymer- water mixture,
2. 10% PHPA Polymer-water mixture,
3. 20% PHPA Polymer-water mixture.

The data collected from experiments were used to determine rheological properties of drilling fluids. The ambient temperature was kept constant, since if the temperature of the fluid samples are varying considerably during the measurements, the rheological properties will be abnormal.

e) Slip velocity calculation with respect to travel length. The slip velocity of the particle was calculated by the ratio t of the particle travel distance l to the time it took to travel. It can be expressed as:

$$v_s = \frac{l}{t} \quad (35)$$

f) Flow rate. The fluid flow rate was calculated from the volume that the fluid filled the cylinder and divided by the time it fills. It can be formulated by:

$$q_f = \frac{V}{t} \quad (36)$$

The example calculations for aforementioned equations are shown in Appendix J

3.3 Test equipment and instruments.

The experimental setup used in this study consists of:

1. For stagnant condition: glass column (39.58 mm inner diameter (ID) and 0.45 m long), plastic column (49.37 mm ID and 0.5 m long), glass column (60.2 mm ID and 0.50 m long), plastic column (78.31 mm ID and 0.35 m long). Different diameter cylinders were used in purpose for defining the wall effect on particle settling velocity.
2. For dynamic condition: plastic column (76.2 mm ID and 1 m long), plastic column (101.6 mm ID and 1 m long), plastic mud tank (capacity 30 liters), rubber hose (25.4 mm ID and 3 m long), rubber hose (25.4 mm ID and 1 m long), a valve (a reliable means of controlling fluid flow rate) (**Figure A-1**)

Schematic drawing of experimental facility is presented in **Figure 7**.

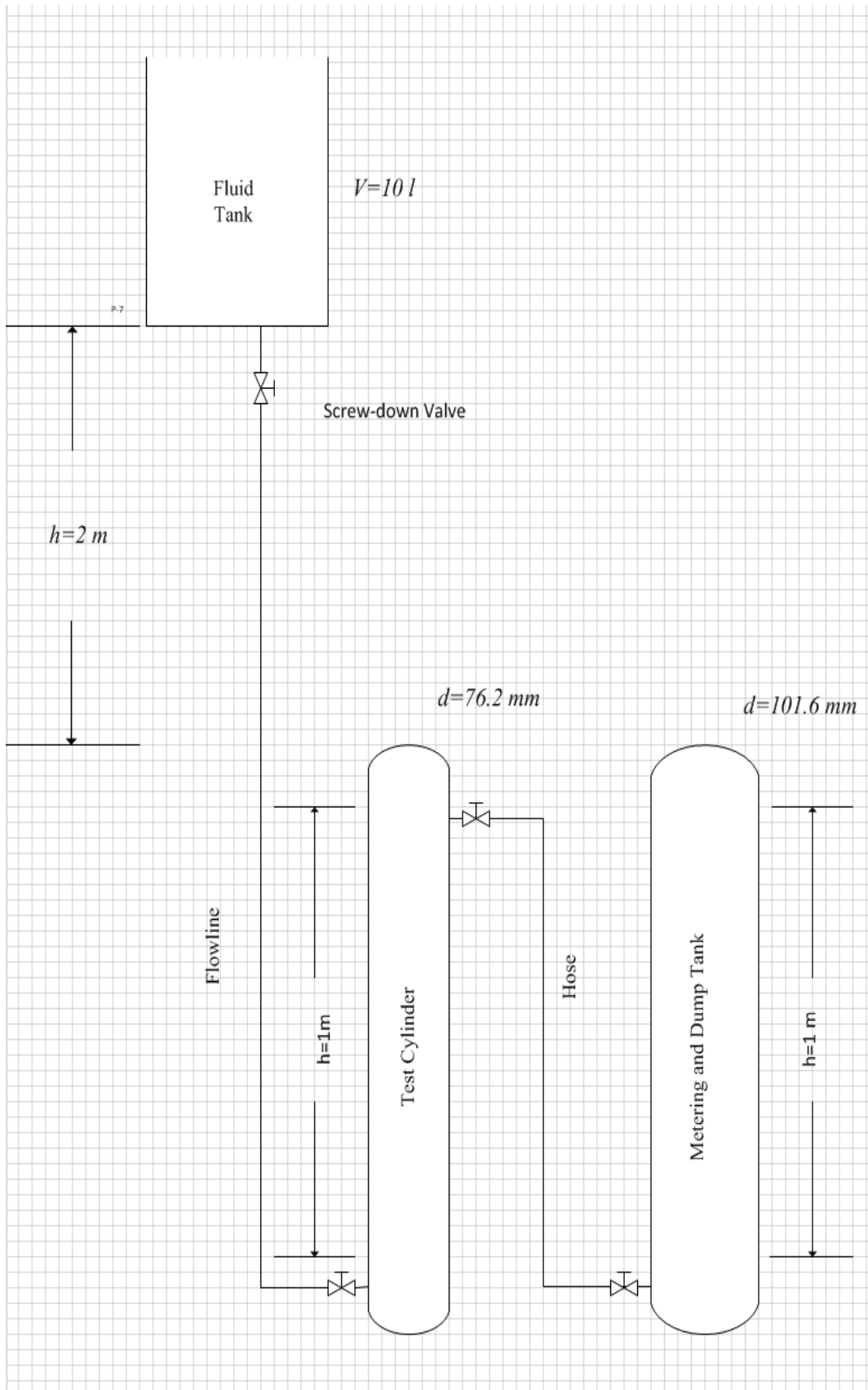


Figure 7. Schematic drawing of apparatus used for measure of cuttings slip velocity in quiescent and at steady state laminar fluid flow (low shear rate)

Viscosity properties: Fann 35 viscometer (**Figure 8**) was used to measure the rheological properties of experimental fluids under room temperature and pressure.



Figure 8. Fann 35 viscometer(Anon 2013).

The test fluid is rested in annular space between an outer cylinder and the bob. The outer cylinder can be rotated at the velocities controlled through gear. This rotation provides fluid motion that applies torque on a bob, which travels through spring and its deflection is read on the scale. Fann 35 viscometer provides rotation at velocities 3, 6, 100, 200, 300, 600 RPM.

Density: Fluid density was measured with using mud balance (**Figure 9a**). It is the most simple and reliable method of determination of mud density. Basically, a cup have to be filled by test fluid and covered with the lid and make sure that no air is entrapped inside and excessive mud is squeezed out. Density will be determined by sliding the slider-weight along the balance beam.

Mixer: Waring laboratory blender (**Figure 9b**) was used to mix the water with polymer powder. It consists of stainless steel container and it rests on a base that contains motor to rotate blades inside the container.



Figure 9. a) Mud balance (left)(Anony. 2013) and b) Waring laboratory blender(right)(Anon 2013).

3.4 Test procedure of slip velocity

Selection of non-spherical particles was done in an arbitrary manner. Visually selected particles were measured on weight-scales and the average particle mass was 0.045 g. A deviation of 0.05 g was allowed in this experiment.

Displacement method was chosen in order to calculate the density of irregularly-shaped particles by conducting the following steps. First, a graduated cylinder was filled with water up to the defined point. Afterwards, weighted amount of particles was dropped inside the graduated cylinder. Increase in volume was observed and noted.

Each time, the particles were screened, weighted, washed and dried before dropping into the cylinder with a fluid.

The tests were carried out in transparent fluids with concentration of 5%, 10%, 20% of PHPA polymer per liter water and plane water. The test fluids were mixed at room temperature in Waring laboratory blender. The viscosity properties and densities of test fluids were checked on Fann 35 VG and mud balance respectively. The fluid rheological properties are presented in **Appendix B (Table B-1, B-2, B-3)**.

All the data collected during the experiment were recorded using a computer program (Microsoft Office Excel).

a) Still-stand fluid-tests

A test started by filling cylinders with experimental fluids. Afterwards, four reference points were drawn on every cylinder. The upper point was 2 cm below fluid level. The length that particles traveled 0.15 cm, 0.2 cm, 0.24 cm were rest of the points. Then, a particle was dropped from the top of the mud column and a stopwatch was used to measure its slip velocity. Each particle was dropped at least five times and the average time of settling was used to calculate the average slip velocity for the study. To allow particles to achieve its constant slip velocity, the particle's slip velocity was measured after a certain length of its free fall. As mentioned above, the length was 2 cm for polymer fluids in all types of columns. The same approach was applied for laminar flow experiment, but with a different length.

b) Laminar flow-tests

The fluid (10 liters) stored in a fluid tank was located on fixed height (3 meters) above the transparent cylinder. The flow (pumping down) was initiated by using a screw-valve. A low-viscous fluid was injected into the test section through a rubber flowline. After constant laminar flow (**Table D-2**) had been set, the particle was released into flow stream by dropping them into the test cylinder. Terminal settling velocity was measured by timing the fall of particle inside a 76.2 ID, 1 meter high glass tube. The slip velocity was timed with a stopwatch. As it was mentioned in the previous section, the allowed length for a particle to reach its constant slip velocity was 5-10 cm.

4. Fluid results (or input data) ahead of the slip velocity test

Fluid design and its properties is one of the essential and important parts of every drilling activity. Properly designed drilling fluid can significantly improve cutting carrying capacity of the mud system. In the following chapters measurements of the rheological properties, dependence on factors such as shaking and mixing time, solubility of polymers and errors related to their measurements will be discussed.

The aim of this section is to analyze and evaluate rheological properties of the water mixture with polymer concentration of 5, 10, 20 gram per liter. Analyzed results will help to design fluid for future research.

4.1 Fluid rheological properties.

The flow curves show that all three drilling fluid samples have different rheological properties (**Figure 10**). In addition, as seen from the figure, the viscosity curve of sample 20%, shifted apart compared to the ones in other fluid samples. However, at low shear rate the viscosity curve of sample 5% coincides with the viscosity curve of sample 10%, but the discrepancy between them increases moving forward in the direction of higher shear rate. All the fluids exhibit shear-thinning behavior, because the fluids resistance to flow decreased with increasing shear stress/ or shear rate.

Since fluid samples do not have yield stress and plot of shear stress versus shear rate go through origin, Power Law fluid model (**Equation 7**) is the most convenient model for samples 1 and 2. Herschel-Buckley model (**Equation 9**) fits for fluid sample 3, since it includes yield point and viscosity depends on shear stress.

However, in order to define effective viscosity for each fluid sample, the Power Law fluid model was applied for all three samples.

Results of the rheological properties for all three fluids samples are demonstrated in **Appendix B (Table B-1, B-2, B-3)**.

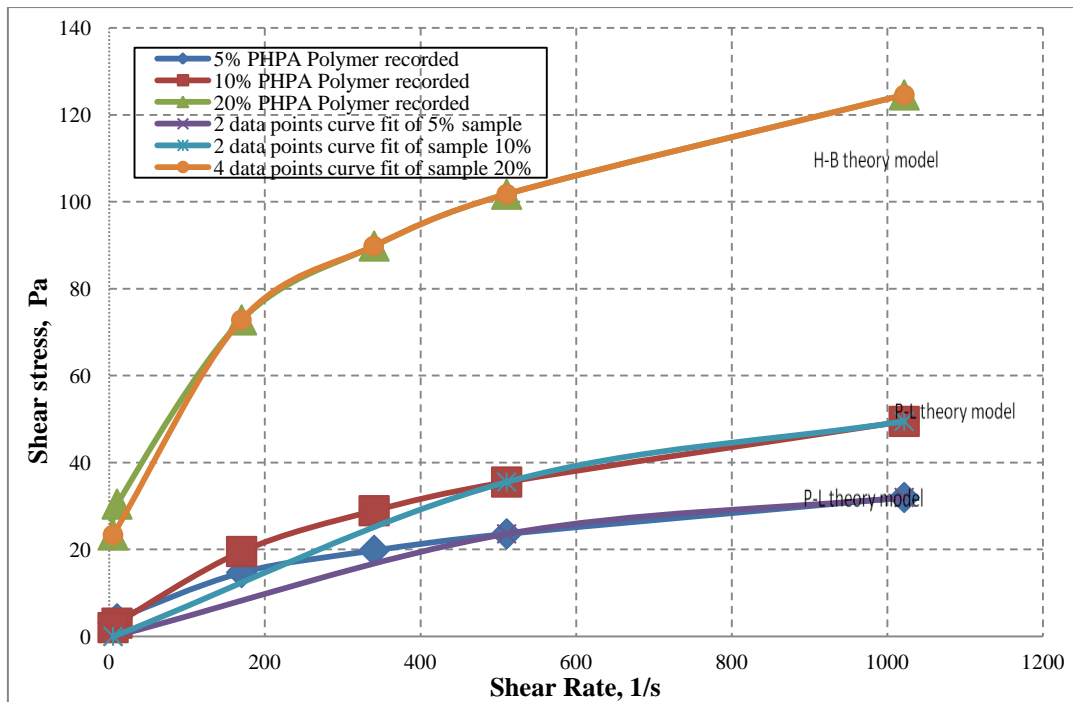


Figure 10. Viscosity curves for all three fluid samples measured with Fann 35 viscometer at ambient temperature and compared with theoretical curves for samples 5% and 10% (based on two upper data points) and for sample 20% (based on four upper data points) are drawn black

4.2 Gel strength

This chapter is aimed to show the dependency of gel strength ability on time and concentration of PHPA polymer. As seen from **figure 11**, all the samples develop gel with time when circulation is interrupted. The values of gel strength recorded at 10 seconds, 1 minute and 10 minutes indicate the strength of the gelation in fluid under static condition.

Another factor is polymer concentration in liquid. The results from the graph, illustrates that presence of PHPA polymer causes increase in gel strength, thus improving suspension of particle in fluid.

While analyzing experimental results (**Tabel B-1, B-2, B-3**), it was noticed that gel strength value of the sample 10% is less of magnitude when compared to sample 5%. To find out the reason for such anomaly, the two additional fluid tests were conducted. These experiments will help to define unexpected behavior of sample 10%.

It should be taken into account that such a fluid behavior was noticed very late and due to lack of time all the results published that in the next chapters were obtained from an experiment on the initial sample 10%.

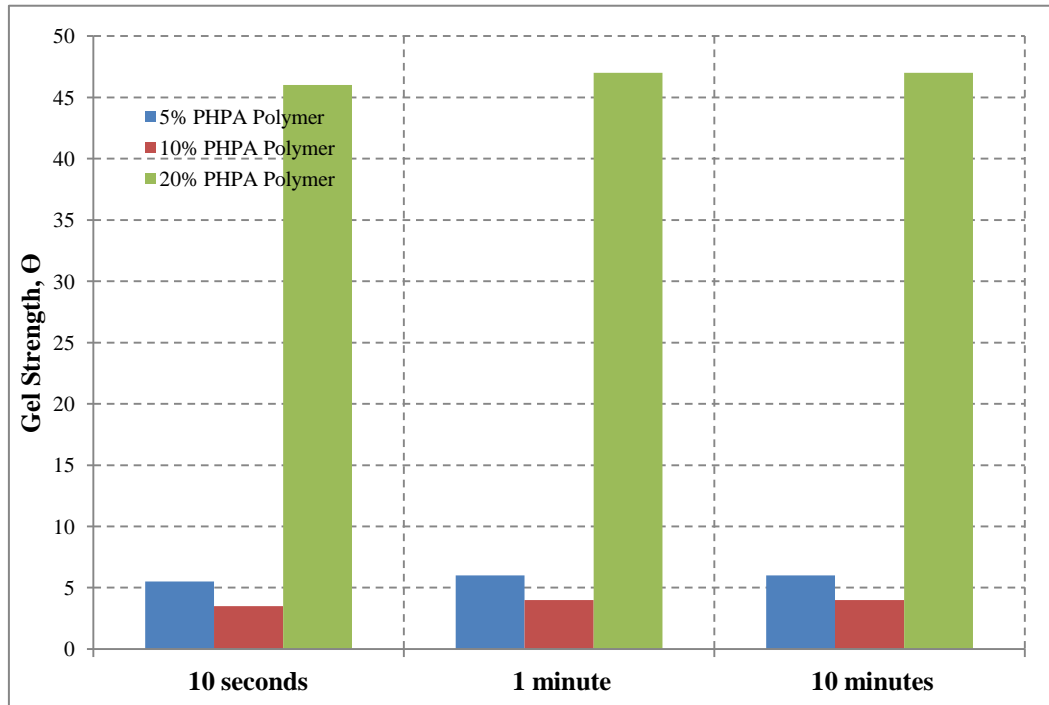


Figure 11. Ten seconds, one minute and ten minutes gel strength measurements for all three fluid samples at ambient temperature

4.3 Polymer solubility in a water medium.

As stated above, the main purpose of this experiment was to analyze the effect of mixing time on rheological parameters. This decision was considered, after careful examination of the sample 10% viscosity curve in region of the low-shear-rate (**Figure 12 and Table B-1, B-2, B-3**) and results of the slip velocities (**Figure 16**).

The four samples of fluid with concentration of 10 gram per liter were prepared. The rheological properties were recorded after 40, 65, 150, 170 seconds of mixing (**Table F-1, F-2, F-3**). **Figure 12** illustrates the trend of changing the properties for different mixing time.

As seen from the figure, fluid rheological parameters change with respect to the mixing time. By allowing fluid extra time to dissolve the polymer, it was noticed increase in rheological properties. The reason for such a behavior was difficulties in dissolving of polymer. Therefore, the polymer needs more time in order to dissolve in water.

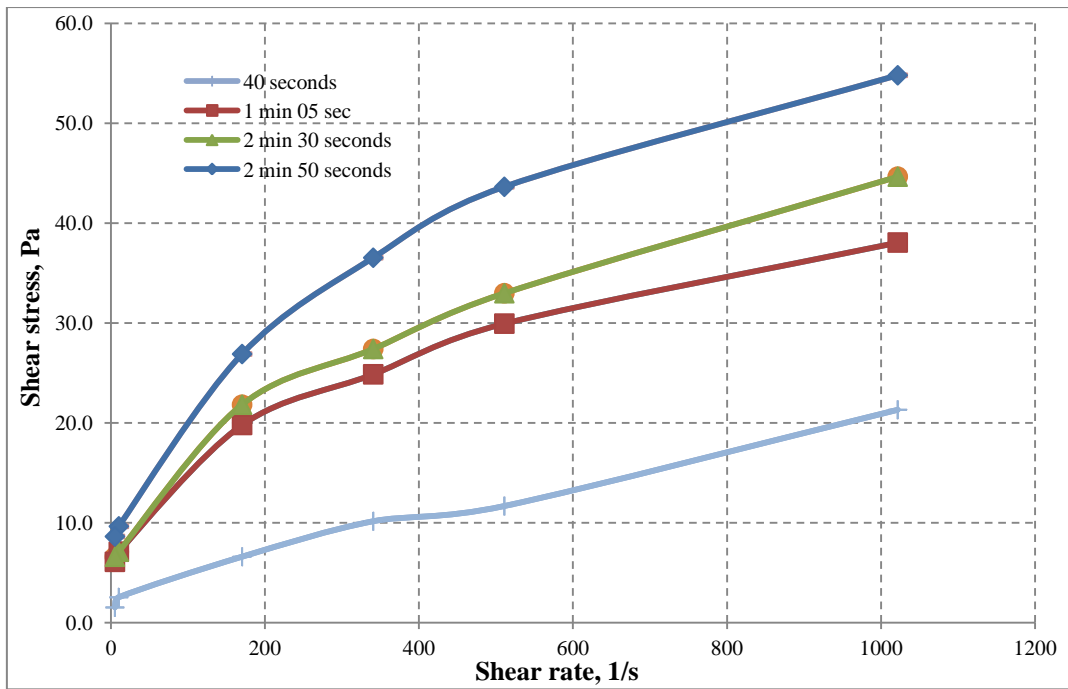


Figure 12. Trend of viscosity curves of four different fluid with 10 gram of PHPA polymer concentration 10 gram per liter of water each with respect to mixing time

4.4 Time-dependency

This test procedure determines the effect of the no-action (or rest) time on fluid parameters. Therefore, it was extremely important to investigate their rheological properties right after mixing, after one day of rest, and after 3 days of rest. Fluid with concentration of polymer 10 gram per liter was used for this study. The (Table G-1, G-2, G-3) presents outcomes of the test.

An accurate study of the experimental results demonstrated that drilling fluids tend to change their properties under no-action time. As seen from the **figure 13**, viscosity curve of right after mixing and one day rest, extremely differs from each other. However, in case of one day and three day rest, the flow curves more or less coincides. The reason for such behavior is that during mixing the link between small molecules (monomers) was broken, which resulted in a low viscosity value of the fluid. However, after some time the bonds bridge or flocculate between monomers which results in gelling and increase in viscosity. Therefore, it is imperative to check fluid properties before conducting experiments.

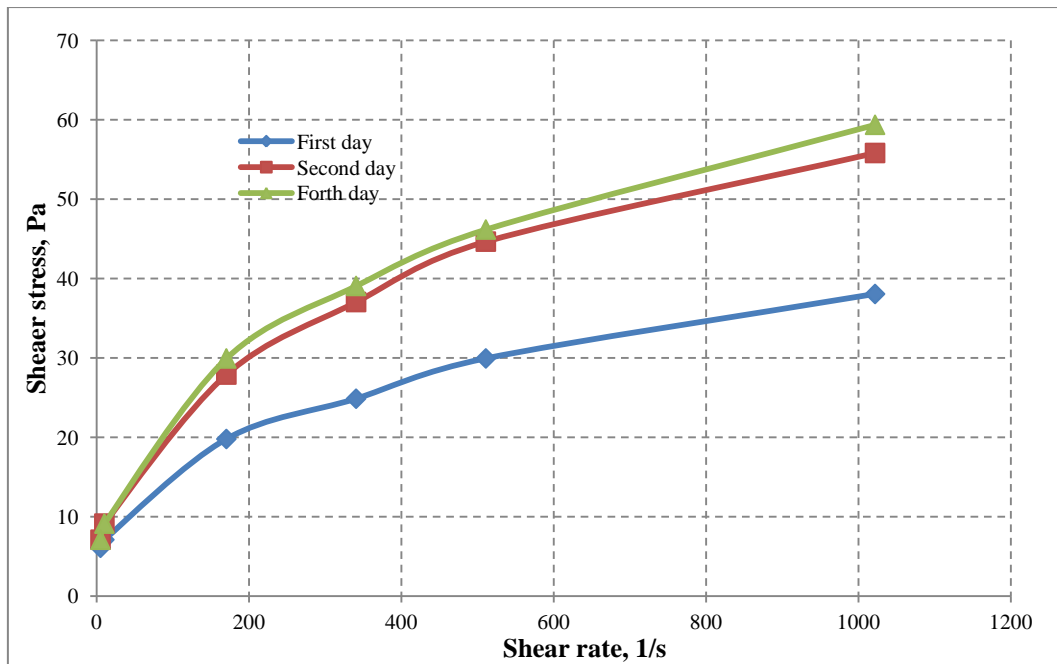


Figure 13. Increase in rheological properties of fluid sample 10% with no-action time (measured immediately, after one and three days)

As seen the change in low shear rate is not that high however at high shear rate the changes is quite noticeable.

4.5 Stirring of fluid just before a new test.

Another factor, which may significantly change fluid rheology is stirring of fluid. As shown on the figure below, fluid is stirred (shaking) for 15 seconds, 30 seconds, and 1 minute before measuring rheological properties on Fann 35 viscometer. As shown on the **figure 14**, there is a significant change between rheology of non-exposed to stirring and 15 seconds stirred fluid. Further experimental results revealed that no matter how long the fluid is stirred, the changes in fluid rheology will not occur, once they have occurred.

Table H-1, H-2, H-3 presents the results of rheological properties for aforementioned conducted tests.

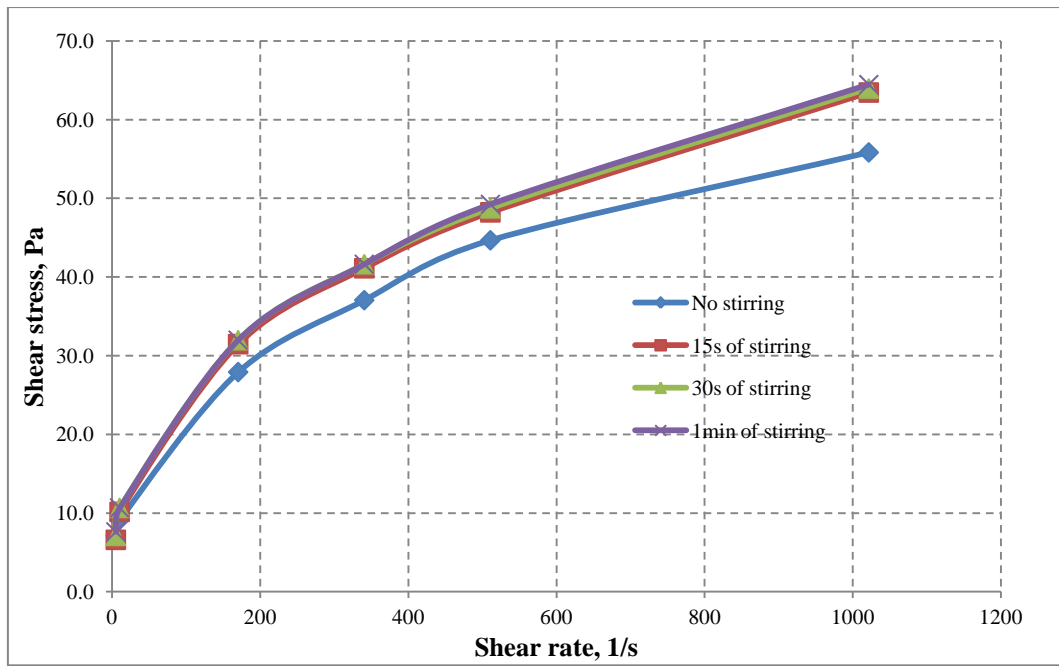


Figure 14. Variation in viscosity properties of fluid sample 10% with respect to the shaking (stirring) time

5. Test results of slip velocity

The following chapter will reveal the influence and the importance of applying low-end-rheology on cuttings slip velocity in quiescent and at steady state laminar fluid flow compared to the more commonly applied standard rheology. The acquired results from experimental and theoretical part were compared in order to derive and evaluate errors. Flow curves, correlation of slip velocity with different variables were plotted and presented in following sections.

5.1 Slip velocities of static condition

This section presents the results acquired from experimental work and theoretical study; the main ideas in these studies were based on static fluid condition. To see the influence of wall effect on cuttings settling, the experiments were done in transparent cylinders with different diameters. The obtained results from experimental study were compared to the calculated theoretical results that used Stokes Law. It was discovered that when particle settled in static fluid, the flow around the particle was in laminar regime.

5.1.1 Experimental results

Settling velocities of various particles measured in the conducted experiments will be presented in this section. In order to find the effect of different variables on particle settling, this chapter categorized into four sections; each section represents particular variable. For better understanding of different variables effect, the obtained results will be discussed using diagrams. The recorded values of settling velocities are outcome of averaging five to ten tries for each case.

5.1.1.1 Wall Effect

Slip velocity vs. tube diameter. The purpose of this experiment was to detect the influence of particle-to-tube ratio on particle slip velocity. Sample 1 and 2 were used as fluid media.

Figure 15 represents correlation of experimentally measured slip velocity with tube diameter for particles of different sizes. In order to emphasize on the difference between velocities, dashed line was drawn on the chart. As seen from the graph, velocity slightly deviate from its initial point in compare to the other velocity results. The highest inclination observed at the point of 49.37 mm. However, despite of all observation, discrepancy in results of all fluids

samples is very small and velocity remains almost at constant value (Table E-1, E-2, E-3, E-4).

Nevertheless, there might be a possibility that cylinders affect slip velocity at some point, since Stokes law assumes an infinite extent (no boundary wall). In other words in order to see any wall effect, the particle diameter should have been close to the pipe diameter in this experiment.

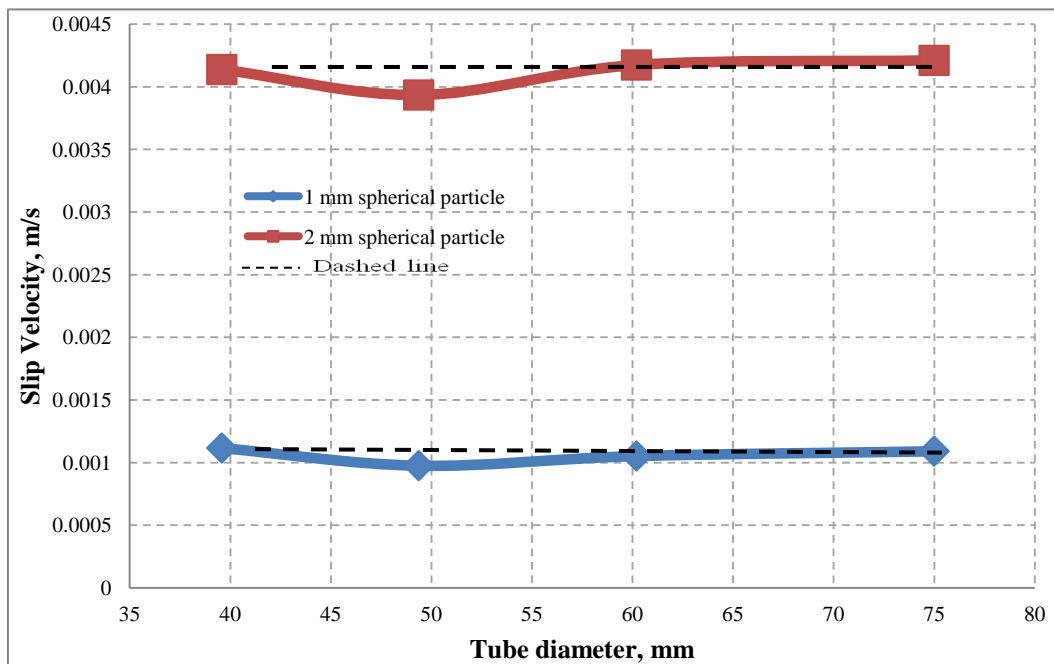


Figure 15. Effect of cylinder wall and annular space on slip velocity of 1 mm spherical particle conducted in fluid sample 5% (Table E-2)

5.1.1.2 Particle diameter and Rheological Properties

The experiment was performed for the reason of establishing correlation between particles settling velocities and their sizes in fluids with different rheological properties. As indicated in Figure 16, the lines pictured on graph describe the rheological properties of fluid samples and points on a plot represent particle size. Other distributed points on chart, represent the non-spherical particle, each in different fluid.

Slip velocity vs. particles diameters. In order to describe the effect of particle size, one non-spherical and three spherical particles of different sizes and sphericities were chosen for running the experiments. Experimental observation showed that the particle settled in fluid at different velocities. It can be seen from figure 16 that the particle of larger size has higher

settling velocity compared to the ones with smaller size. Hence, slip velocity of particles is directly proportional to the size of particles. The experimental test results of slip velocities for all particles conducted in all three fluid polymer concentrated samples and water are shown in **tables E-1, E-2, E-3, E-4**.

For non-spherical particle, average particle diameter and sphericity were determined to be equal 3.387 (**equation 32**) and 0.91 respectively.

Slip velocity vs. rheological properties. Another factor influencing particle settling velocity is effective viscosity of fluid sample. The effective viscosity is mainly dependent on shear stress created during the settling of particles. Experiments showed that slip velocity of the particles with the same size is dependent on the fluid samples of different rheological characteristics.

Illustration in **figure 16** confirms the fluids behaviors mentioned for different samples in previous section. It shows the effect of rheological parameters of fluids on particle slip velocity. As seen from the graph, spherical and non-spherical particle settled slower in the higher fluid viscosity parameters (e.g. for sample 3, $K = 16.5$, $n = 0.292121$). The fastest settling occurs in fluid sample 2, while the weight of polymer in sample 2 was higher than in sample 1. **Figure 16** and **Tables E-1, E-2, E-3** show that an increase in flow behavior index, n , increases (**Table B-1, B-2, B-3**) the effective viscosity for a considered shear rate but decreases slip velocity. However, since the flow consistence index K is not constant for all three samples, this statement cannot be always true. Another reason for this peculiar behavior might be the effect of gel strength. Since, fluid in stagnant state and shear stress applied to break gel strength the particle settles. Hence, increase in rheological properties of fluid while maintaining other variables resulted in a decrease of particle slip velocity.

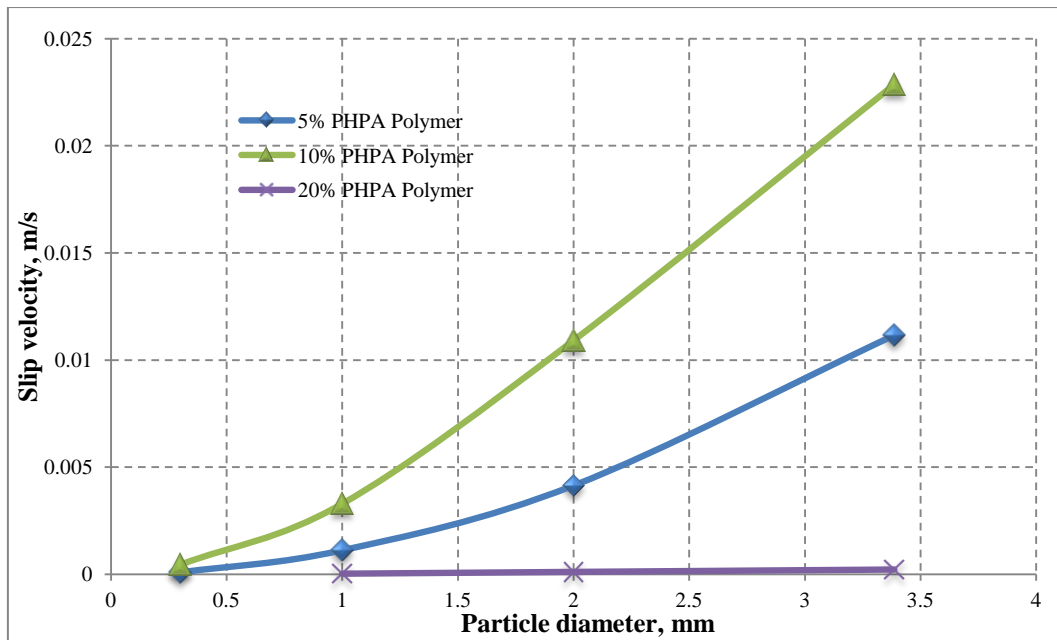


Figure 16. Effects of all three fluid samples rheological properties and particle size on particle slip velocities.

5.1.1.3 Travel length

Slip velocity vs. free-fall distance. The aim of this experiment was to find out any changes in particle settling velocity at all observation points of the cylinder and the on-set of the terminal settling velocity. These points were located at different distances from a predetermined point called starting point.

To examine the effect of free-fall distance, fluid samples 1 and 2 were used. **Figure 17** illustrates the results for settling velocity of spherical particle size of 1 mm and 2 mm, that settled at given fluid parameters (sample 1) $K = 1.5$ and $n = 0.438121$. As seen from the figure, slip velocity of particle with 1 mm diameter shifts between 0.001148 m/s and 0.001181 m/s (**Table E-5**). The drawn dashed line confirms that the trend of these points lies on a straight line. As for the other sample with the diameter of 2 mm, slip velocity value for the last point deviates from the straight line. Fluid velocity for this particle varies between 0.004308 m/s and 0.004545 m/s (**Table E-6**). However, despite the fluctuation in velocity, it is negligible in compared to the rest of other particle slip velocity.

The theoretical analysis and observation showed that the particles reached their terminal settling velocity before they approached start-measure line. It shows that the manual recording technique of the recorder was trustworthy and repeatable.

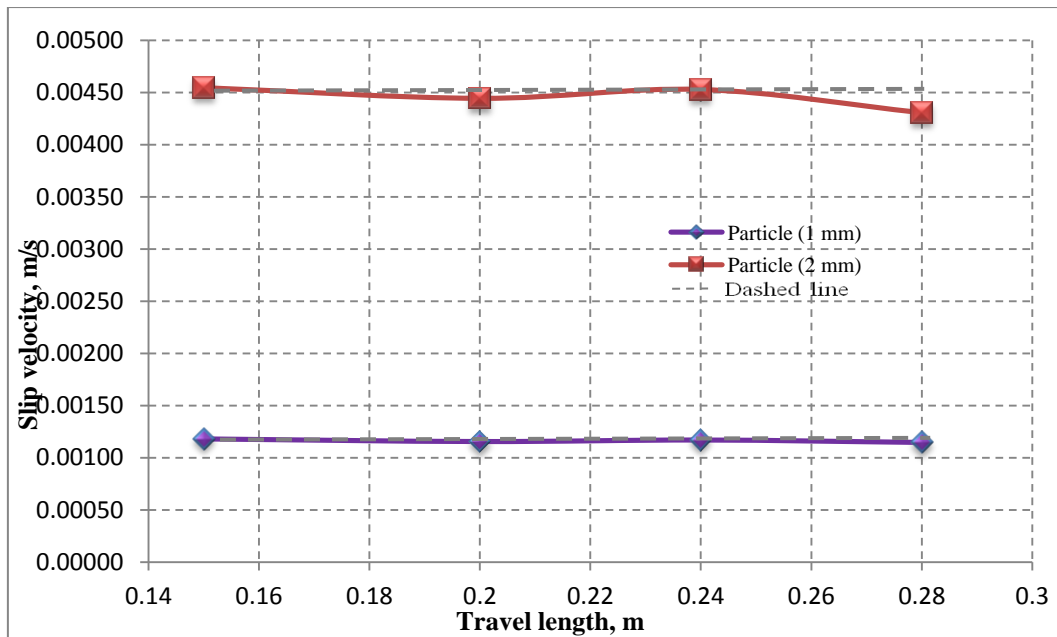


Figure 17. Change in particle slip velocities of 1mm and 2 mm particles size in fluid sample 5% with respect to travel length.

5.1.2 Theoretical results.

In any experimental study, any desired value should be evaluated in terms of other variables. As for this experiment, slip velocity was calculated as a function of particle size, and rheological properties. This chapter introduced in order to evaluate the accuracy of the Stokes Law.

5.1.2.1 Drag coefficient

Drag coefficient vs. Reynolds number. The approach used in this section was to determine the relationship between drag coefficient and particle Reynolds number evoked from the plot. The particle Reynolds number and drag coefficient were calculated by using **equation 20 and 21** respectively.

Constant slope on the graph represents laminar flow and the points in the graph clear the correlation of drag coefficient with particle Reynolds number (**figure 18**). Normally, the flow enters from laminar to the transition region after the particle Reynolds number equal to one. This fact validates the plot. According to the previous analyses, a particle tends to settle at low slip velocity in laminar flow region, which offers the greatest possible resistance (drag coefficient) in this flow regime. Thereby, it can be concluded that drag coefficient is inversely proportional to particle Reynolds number.

The data, acquired from calculation as mentioned above (**Table C-1, C-3, C-4**), were compared with data points acquired from published analyses. In order to confirm the value an experimental correlation chart from “Applied Drilling Engineering Book” (A.T. Bourgoyne Jr, K.K. Millheim et al. 1986) was utilized. These data (**Table I-1**) were taken from the graphical illustration that demonstrates the correlation between drag coefficient and particle Reynolds (**figure 6**). If we look at the chart, we will see that friction factor is plotted against particle Reynolds number. E.g., if particle Reynolds number is equal 0.4, we go perpendicularly upwards parallel to the y-axis until the friction factor (drag coefficient) of value equal to 60 is met. The point where intersection occurs is used for finding sphericity of the particle. As seen from the graph experimental and theoretical points were distributed homogeneously around the related trend line showing laminar flow. From this, it can be deduced that theoretical equation and experimental observation are consistent.

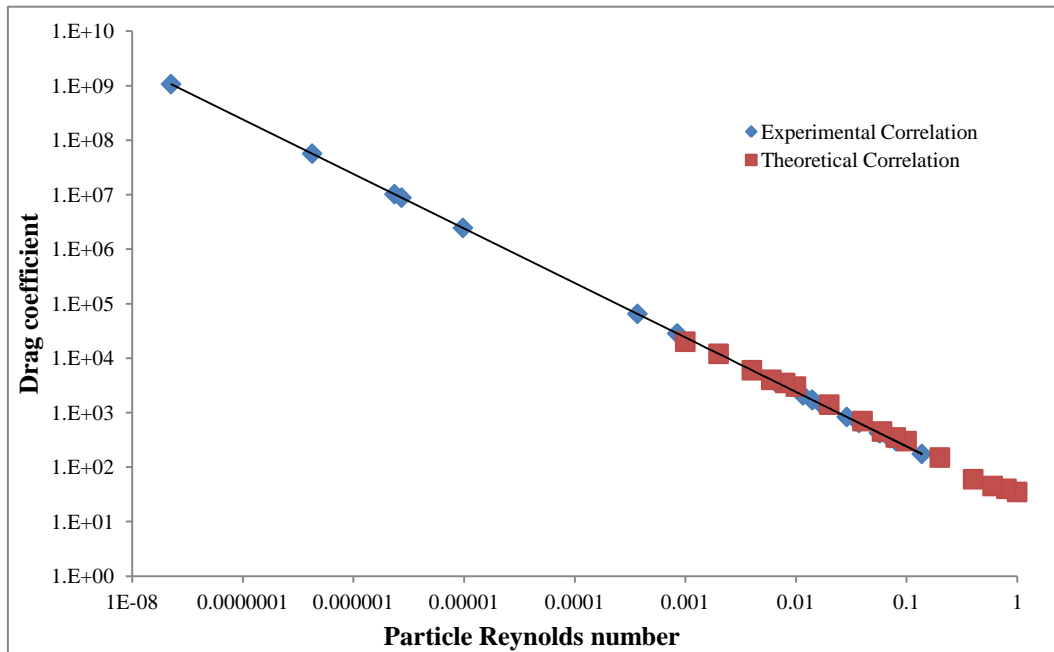


Figure 18. Experimental correlation of the drag coefficient with the particle Reynolds number for all three fluid samples in laminar flow compared with the published drag coefficient versus particle Reynolds number

5.1.2.2 Reynolds number

Slip velocity vs. Reynolds number. Another method used to define flow around the particle is to build the relationship between particle slip velocity and its Reynolds number. From correlation of aforementioned parameters it is clearly seen that particles settled in laminar flow regime (**Figure 19**). It is also proved (A.T. Bourgoyne Jr, K.K. Millheim et al. 1986),

according to the published analysis from the Applied Drilling Engineering (A.T. Bourgoyne Jr, K.K. Millheim et al. 1986), that the laminar flow border ends at particle Reynolds number equal to one.

As seen from the figure, at viscosity parameters of sample 5%, $K = 1.5$ and $n = 0.438121$ (**Equation 9**), the lowest Reynolds number 0.00002 were estimated for 0.03 mm size particle (**Table C-1**). For the non-spherical particle 3.387 mm of sphericity 0.91, the particle Reynolds number were equal to 0.06 (**Table C-1**). The constants K and n of the power law model used to describe fluid parameters were calculated from the **equations 8 and 9** respectively.

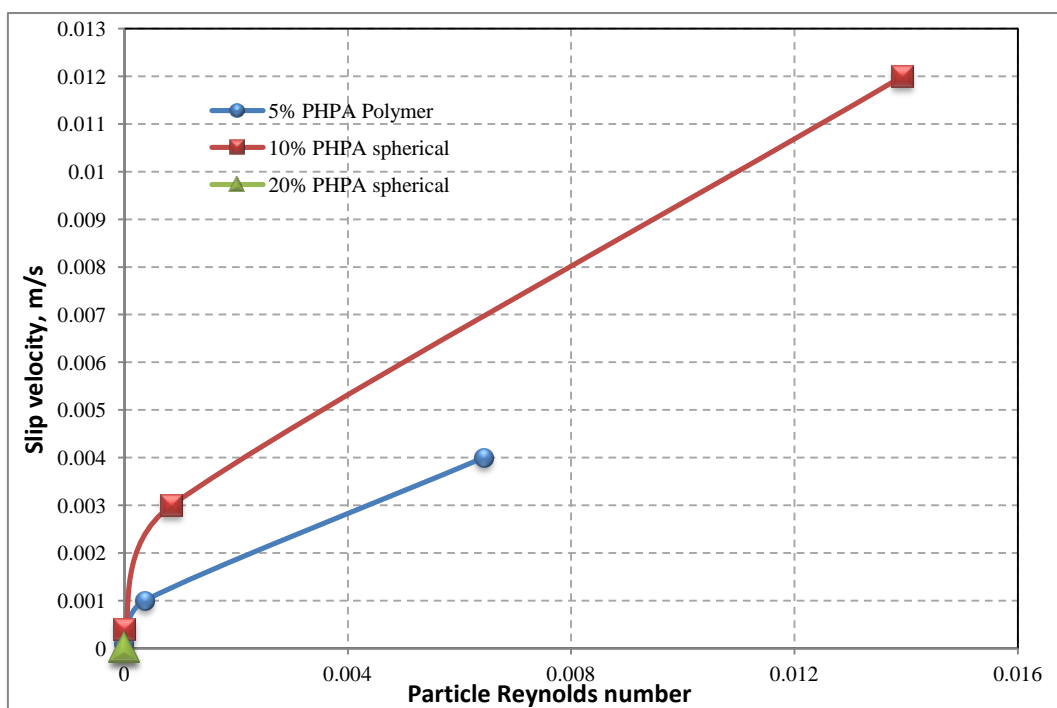


Figure 19. The correlation of slip velocities with particles Reynolds number for all three fluids samples

5.1.2.3 Particle diameter

Reynolds number vs. particle diameter. The results presented below show correlation of particle Reynolds number with particle diameter. Presented results were evaluated in low viscous fluid sample 5% with parameters $K = 1.5$ and $n = 0.48121$ (**Table C-1**).

As seen from the **figure 20**, increase in particle size, increases particle Reynolds number. Since larger particle settle in fluid faster, the particle Reynolds number increases. At small sizes the slope between particle size is more smooth and parallel, however, as the particle

diameter increases, the line between them gets more perpendicular. **Table C-1, C-3, C-4** demonstrates the results for Reynolds number calculated for all three fluid samples.

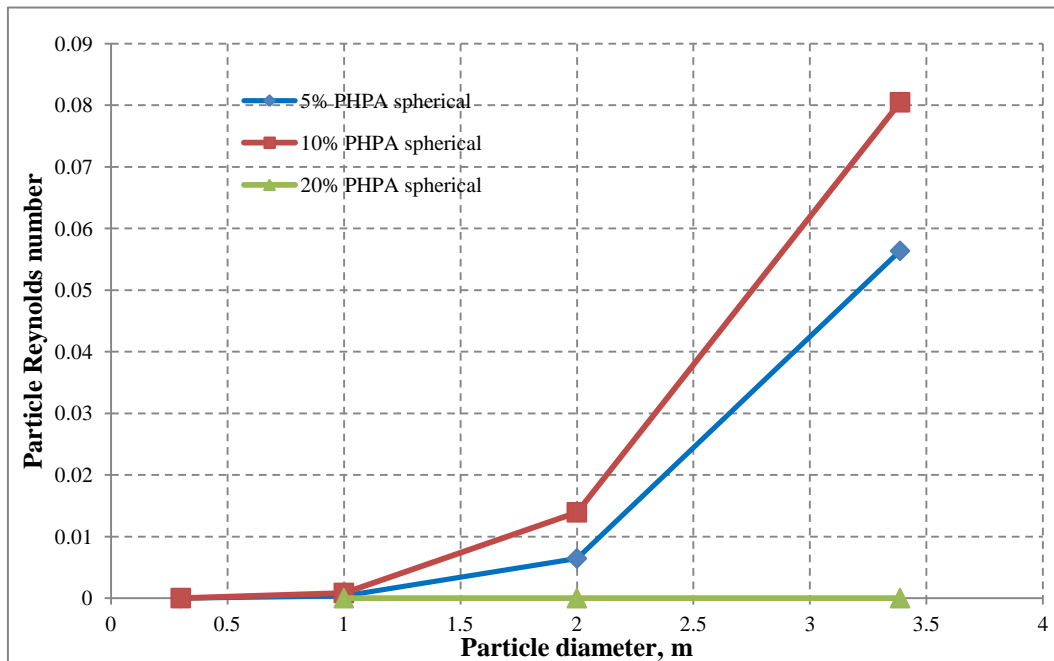


Figure 20. Correlation of particle Reynolds number with particle size in all three fluids samples

5.1.3 Comparison

Observed slip velocity vs. calculated slip velocity. Sensitivity analysis of all results (**Table C-1, C-3, C-4** and **Table E-1, E-2, E-3**) conducted in this section, allowed to evaluate the accuracy of the Stokes Law (**equation 19**) with respect to experimental observation. In order to reveal the relationship between these velocities, the correlation between them is illustrated in **figure 21**.

As shown in the figure, the velocity data points are equally distributed throughout the range of velocities. The trendlines and points used in chart represent agreement between velocities.

From analysis of the slip velocities of the solid particle, it was found that correlated results closely agree or had errors less than 100% (**Table C-1, C-3, C-4**). For instance, it can be noted that the error for the sample with small particle size (0.3 mm) lies within the range of 70 percent up to 87 percent while decrease in rheological properties occurs. For medium size particle (1 mm) error span estimated to be between 85 percent and 43 percent with decreasing

rheological properties. As for the bigger particle size (2 mm), the error value decrease from the 75 percent to approximately 16 percent with decreasing rheological properties.

Hence, it is easy to correlate the velocity results of a big-size particle at low viscous fluid.

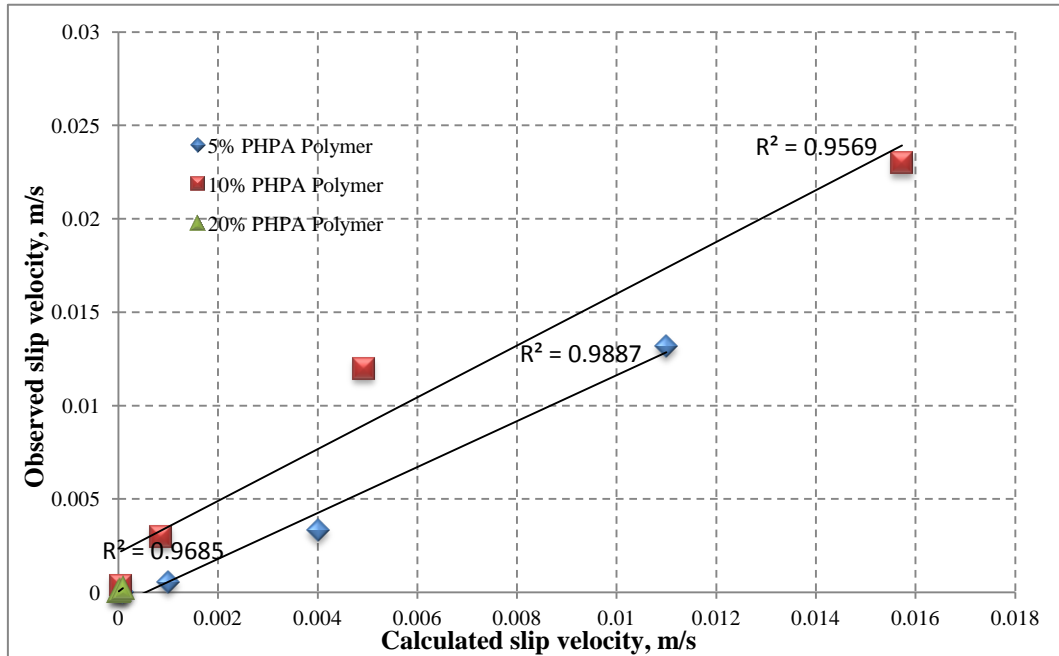


Figure 21. Comparison between observed and calculated slip velocity for all particle size in all three fluid samples

5.2 Slip velocities of dynamic condition

All the previous experimental results were acquired for stagnant fluid. However, in this section the particle will settle while liquid is flowing at a very low velocity in vertical direction. In order to reproduce this process, the experiment was conducted while the fluid was flowing at various flow rates (Table D-1, D-2).

5.2.1 Flow dependence

Slip velocity vs. particle size. The objective of this chapter is to show the influence of flowing fluid compared to stagnant condition. The data on Figure 22 represent the results that reveal the influence of flowing fluid.

Consider a given sample with 5-gram polymer concentration per liter of water (Table B-1) with different particle sizes of 1 and 2 mm, which is subjected to static and dynamic conditions. The comparison of obtained values (Table C-1, Table D-1) illustrated in figure

23 shows that the slip velocity for both flow conditions increases as particle becomes larger. In addition, the trend of slip velocity increase in stationary condition is approximately twice as large as a dynamic one. The reason for a smaller value of dynamic condition trend line slope can be interpreted by the resistance of stream flowing in the opposite direction of particle settling.

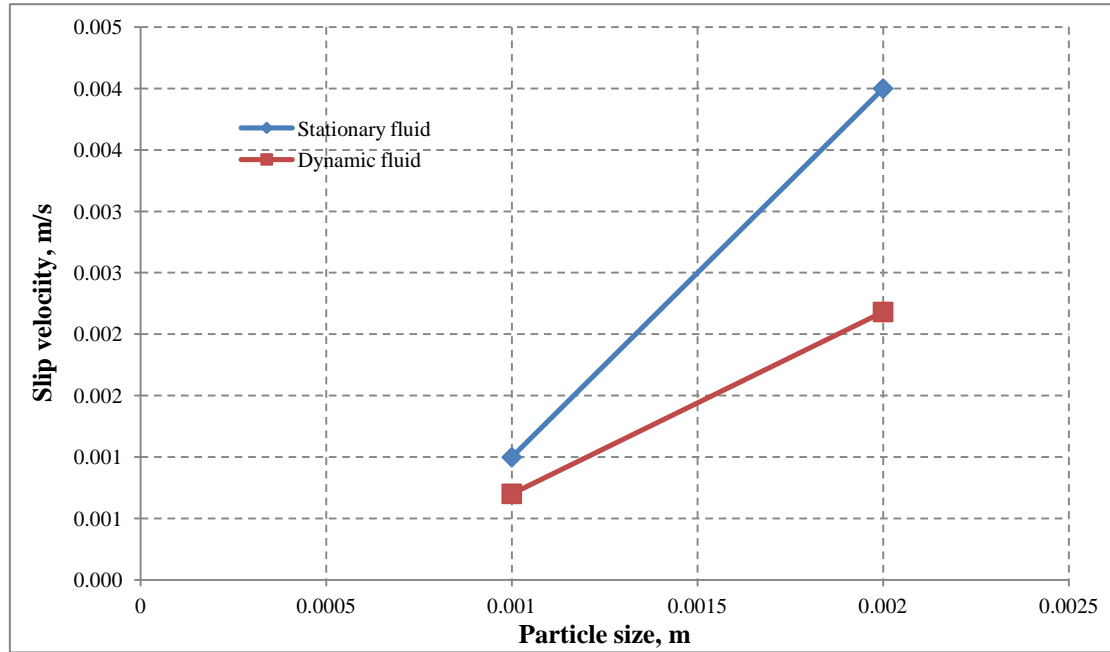


Figure 22. Comparison of the slip velocity results in stationary and dynamic fluid conducted in mixture of 5 gram PHPA polymer per liter water

5.3 Comparison

Shear rate provided by particle slipping is of great concern in this analysis. As discussed in section 2.3.5, proposed different shear rates. In this section, presented the results of slip velocities obtained from the experimental tests and theoretically calculated by using different shear rates equations. The tests were conducted in fluid sample 5% and theoretical calculations consider its rheological properties (**Table B-1**).

As seen from the graph, all results differ from each other. For 0.3 mm and 1 mm size particles, $3v/d$ equation give less per cent of error 4% and 16 % respectively (**Table C-2**). For 2 mm spherical and 3,387 non-spherical size particles, v/d is the most accurate equation in predicting shear rate values (**Table C-1**). The error values reach 16 % and 20 % respectively.

Based on analysis and results presented on **figure 23**, v/d remains as a suitable equation for predicting shear rates of the slipping particles, since the curves overlay.

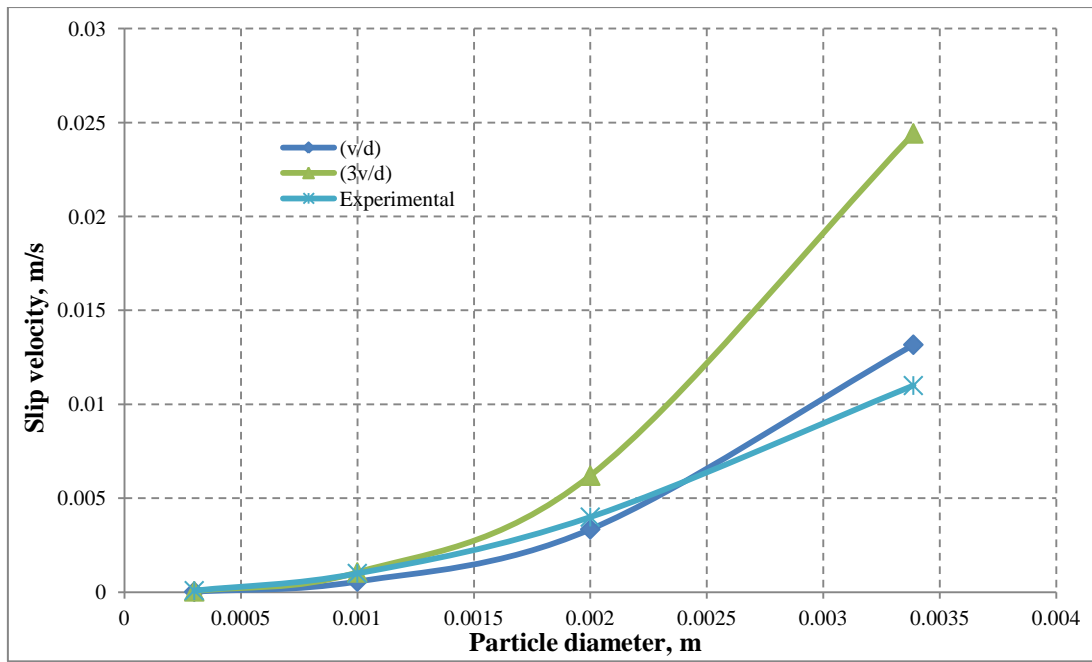


Figure 23. Comparison of theoretically proposed shear rates around particle with experimental results in fluid sample 5%.

6. Discussion

The main purpose of this study was to define through taken experiments the significance of the low-end-rheology and to develop an understanding of its influence on particle slip velocity at stagnant and steady state laminar fluid flow instead of standard Newtonian rheology (water). In addition, extensive evaluation has been carried out on an applicability of the Stokes Law equation and evaluation of the errors for given rheology.

Slip velocity is another important parameter, which was thoroughly investigated during the experiments and subsequent calculations. There were some unexpected results regarding slip velocity, which are also reported in detail in related sections of the study.

Besides, the recommendations for the future researches/studies will also be given at the end of this chapter.

It is shown in the beginning of the thesis that the whole work is divided into three steps::

1. Obtaining knowledge based on previous researches
2. Planning and conducting the experiments
3. Evaluation of obtained results.

It is possible, that during experimental work some errors might occur. Taking into account that there is also time limitation in taking the experiments the possibility of errors is higher, as more time is needed to gain more experience about and conduct the experiments without any errors. In the next section, it will be also discuss all the shortcomings of the experiment.

6.1 Discussion of Fluid tests

One of the essential parts of this study was the preparation of fluids for the experimental investigations of particle slip velocity. Observation of the experiments demonstrated, that fluid rheological properties were greatly affected by the fluid mix time and hydration time after mixing. It was expected, since time is required for polymer to be dissolved in fluid. Nonetheless, it was not anticipated, that even after long and proper mixing, fluid may also change its viscosity, if it is mixed again after more mixing time. Therefore, fluid mixing time is different for all three fluid samples, since high concentration of polymer in liquid is hard to dissolve.

Based on the obtained results, it was revealed that fluid tended to change its rheological properties even with no-action time (rest time). This phenomenon was discovered after evaluation of the results on particle settling; it was manifested that particle slip velocity has higher magnitude in 10% PHPA polymer concentration in comparison with 5% PHPA polymer concentration. Since experiments were conducted at different times after fluid preparation, it induced inconsistency in results of slip velocity and led to significant the errors. Nevertheless, in order to verify the aforementioned statement, the trial experiment with evaluation fluid no-action time (waiting time) was performed at different time span. The acquired result confirmed that no-action time is one of the reasons of change in fluid rheology.

Another factor, which resulted in change of the rheology was shaking of fluid prior to conducting experiments on slip velocity. Since during the experiment fluid were poured in cylinders, it stirred (sheared) the fluid and led to changes in rheological properties of the fluid.

6.2 Discussion of Experimental set-up

During the test, experimental device demonstrated a weakness, which initially has been restricted to measure particle slip velocity. As it was planned, the flow rate was set-up by means of valve and difference of height between flow tank and test cylinder, in order to provide steady-state laminar flow throughout the test. However, during the experiment, it was impossible to maintain constant flow rate of fluid in measuring and dump cylinder as was initially planned (**Figure 9**). Firstly, due to a low weight of particle, it tended to travel into direction of the stream. Eventually, it was decided to drop the particle before it starts to flow into the dump tank and measure flow rate in test cylinder.

Another factor, which caused difficulties in determining the flow rate of fluid was the limited amount of fluid volume and capacity of the dump tank. While all fluid was run out in flow tank, fluid in flowline was a means of liquid supply. By decreasing the liquid in flowline, the height between fluid level in flowline and test cylinder decreases. This led to the change in hydrostatic pressure, which in turn affected the flow rate of the fluid. Eventually, it resulted in change of particle slip velocity.

6.3 Discussion of the error related to the experimental results

In fact, the slip velocity estimation is a crucial part of this study, since it estimate of usefulness of the low-end-rheology, cuttings transport or hole cleaning. Several factor have been discovered during the theoretical study and verified while performing experimental investigation. To experimentally define the influence of low-end rheology two types of experiments were conducted: static and dynamic. The first test type was utilized in order to estimate the slip velocity of particle in low-end-rheology and then compare it to measured slip velocity of standard rheology. Rheology was selected on the basis of compared results of slip velocity and was considered as a optimum rheology.

Second type of investigation was to see particle velocity behavior by dropping a particle in flowing mud at steady state condition. However, the weakness were discovered for both of cases.

Slip velocities measurements from the experimental tests demonstrated that particle velocity in sample 10% gave higher slip velocity than it was expected. Since slip velocity of 1mm particle in sample 5% and sample 20%, the average velocity were 0.00112 and 0.00003 m/s respectively. It was expected to have velocity somewhere around between, due to 10% of polymer concentration. However, while analyzing the experimental data it was noticed that the average slip velocity of 10% sample was equal to 0.003 m/s, which is much higher than it should be if we compare to the sample 5%. This unexpected behavior refer to all particles (in terms of size).

Another interesting factor is fluid settling velocity in dynamic and static conditions. Initially, it thought that particle in dynamic flow will settle at higher velocity rate in compare to the static condition. Because, it was assumed, that due to particle falling and fluid flow, the fluid will be subject to the higher shear rate which in its turn affects to slip velocity (equation) and will be resulted in faster settling. However this conception was erased, when it was experimentally observed that particle in dynamic flow settled slowly. The reason for this is that in dynamic flow there is fluid flow, which provides resistance for settlement of the particle in dynamic flow and of course, another reason for this is also effective viscosity. However, in static you don't have flow, and resistance is provided by means of effective viscosity.

The results of slip velocities gained from experiments and theoretical results were calculated in terms of two different shear rates equations. The comparison of these results reveals, that choice of the equation plays important role on predicting of particle slip velocity by applying Stokes Law. The equation of shear rate proposed by Daneshy ($3v/d$) is showed very accurate prediction of slip velocity at particle size of 0.3 and 1 mm of sphericity 1. However, as the particle size gets bigger and sphericity of the particle decreases, the equation shows limitations\ in providing of accurate results (**Figure 24 and Table C-2**)

Another equation of shear rate suggested by Novotny (v/d) demonstrates relatively accurate results at particle on all three particles sizes of sphericity 1. However, as the particle size gets bigger and sphericity of the particle decreases, the resulted equation shows decrease of error value down to 32% (**Figure 24, Table C-1**).

Comparison of the theoretically and experimental results demonstrated that Stokes Law equation is by far the appropriate for determination of particle settling velocity, but it has also may give errors. The correlation of the results showed that Stokes Law gave the least error values for fluid sample 5% and highest for sample 20%. Hence, as the concentration of polymer increases the Stokes Law equation loses its ability to accurately predict slip velocity of the particle.

7. Conclusion

Measured slip velocity of spherical and non-spherical particles under static and steady state laminar condition differ considerably from the slip velocity when applying the standard rheology (water) and low-end-rheology. Compared results of slip velocities showed that particle transport based on low-end-rheology is much closer to observed slip velocity rather than calculated by high-end. The present study was designed to determine the effect of low-end-rheology on particle slip velocity. The following conclusions are made from the analysis of the results acquired during the current study:

- An increase in the viscosity of the static fluid was found to decrease the settling velocity for spherical and non-spherical particles when comparing low-end-rheology and standard rheology.
- The steady state laminar flow improves the carrying capacity, since it decreases particle slip velocity compared to the stagnant condition of the same rheology.
- Cuttings size had a great impact on particle slip velocity, both in stagnant and at steady-state laminar flow.
- Non-spherical particles have the same slip velocity as corresponds to effective diameter as spherical.
- Measuring a particle velocity at four different positions allowed to conclude that the particle settles at a constant slip velocity.

Some observations were initially anticipated. It was not a surprise to see that fluid flow rate improved carrying capacity of investigated fluids. It was also observed that gel strength played a crucial role in particle settling velocity.

Overall, the study met the expectations and some important conclusions were made based both on theoretical research and conducted experiments.

8. Recommendation

This research was a pre-study, which will help to perform a more detailed and deep investigation to evaluate the influence and importance of low-end-rheology in the oil industry.

Due to time limitation, it was not possible to fully evaluate the results or work with the errors.

A deep study has to be performed with different variables (e.g., inclination, eccentricity, pipe rotation, various sphericities, etc) and more sophisticated device.

However, some recommendations will be given in order to contribute to future progression and allow the person who will conduct this kind of experiment to avoid same errors.

Below are some suggestions, which could be useful if a similar study is going to be performed.

- Prior to commencing the experiment check and record fluid rheological properties
- Make sure that polymer is mixed in the fluid (allow at least 4-5 minutes mixing time)
- Conduct experiments with various particle sphericity and sizes in order to obtain more reliable results
- Perform a check run to see effects of temperature on polymer rheology

It is also recommended to have a flow meter, which makes the flow rate measurement much easier. Flow rate is a crucial part of this type of experiments and any changes without proper recording can result in wrong calculations and, hence, incorrect conclusions.

The surface where the equipment is installed has to be smooth and even, otherwise slip velocity measurements can be affected.

If there is a choice use another type of equipment as this apparatus is quite robust to operate due to some design limitations, which do not allow to perform proper particle drop.

Abbreviation

PHPA	Partially hydrated polyacrylate
ROP	Rate of penetration
RPM	Revolution per minute
ESD	Equivalent spherical diameter
YP	Yield point
ID	Inner diameter

Nomenclature

τ - shear stress

τ_o - yield point

γ - shear rate

γ_w - shear rate at pipe wall

γ_t - total shear rate

γ_f - shear rate imposed by fluid movement

μ - viscosity

μ_a - apparent viscosity

μ_{pl} - plastic viscosity

μ_{eff} - effective viscosity

θ_{300} - reading at 300 RPM

n - flow behavior index

K - consistency index

λ - particle-to-tube diameter

f - wall factor

ψ - sphericity

g - gravity acceleration

v - velocity

$v_2 - v_1$ - velocity difference between fluid layers

v_s - slip or settling velocity of particle

$v_{s,f}$ - slip velocity in confined medium

$v_{s,\infty}$ - slip velocity in infinite extend

v_a - annular velocity

q_f - fluid flow rate

d_{dp} - drillpipe diameter

d_p - particle diameter

d_{ESD} - equivalent spherical diameter

$d_2 - d_1$ - difference in diameter between two points (locations)

h - disc thickness

l - length

A - area

V_p - particle volume

t - time

ρ_p - particle density

ρ_f - fluid density

m_p - particle mass

F_g - gravity force

F_b - buoyancy force

F_d - drag force

F_f - friction factor

C_{drag} - drag coefficient

N_{Re} - Reynolds number

1,2,3 - number of measurements

References

- A.T. Bourgoyne Jr, K.K. Millheim, M.E. Chenevert and F. S. Y. Jr. (1986). Applied Drilling Engineering, Society of Petroleum Engineers.
- Alcocer, C. F., A. Ghalambor and L. H. Sweet (1992). A STUDY OF RHEOLOGICAL PROPERTIES OF NON-NEWTONIAN FLUIDS AND SETTLING BEHAVIOR OF CERAMIC PROPPANTS MANUFACTURED IN LOUISIANA, USA. SPE Latin America Petroleum Engineering Conference. Caracas, Venezuela, 1992 Copyright 1992, Society of Petroleum Engineers, Inc.
- Anon (2013). Fann Viscometer.
- Anon (2013). Laboratory Blender.
- Anony. (2013). Mud Balnace.
- Chien, S.-F. (1969). ANNULAR VELOCITY FOR ROTARY DRILLING OPERATIONS.
- COSMOS (2008). Online Solutions Manual Organisation System.
- Daneshy, A. A. (1978). "Numerical Solution of Sand Transport in Hydraulic Fracturing." Journal of Petroleum Technology **30**(1): 132-140.
- Di Felice, R., L. G. Gibilaro and P. U. Foscolo (1995). "On the hindered settling velocity of spheres in the inertial flow regime." Chemical Engineering Science **50**(18): 3005-3006.
- Fang, G. (1992). An Experimental Study of Free Settling of Cuttings in Newtonian and Non-Newtonian Drillings Fluids: Drag Coefficient and Settling Velocity, Society of Petroleum Engineers.
- Ford, D. J. (2003). Drilling Engineering.
- Herzhaft, B., L. Rousseau, L. Neau, M. Moan and F. Bossard (2002). Influence of Temperature and Clays/Emulsion Microstructure on Oil-Based Mud Low Shear Rate Rheology. SPE Annual Technical Conference and Exhibition. San Antonio, Texas, Copyright 2002, Society of Petroleum Engineers Inc.
- HOPKIN, E. A. (1967). Factors Affecting Cuttings Removal During Rotary Drilling.
- Hughes, B. (2006). Drilling Fluids.
- Krumbein (1939). The Role of Hydraulic Laboratories in Geophysical Research at the National Buroau of Standards.
- Larsen, T. I., A. A. Pilehvari and J. J. Azar (1997). "Development of a New Cuttings-Transport Model for High-Angle Wellbores Including Horizontal Wells." SPE Drilling & Completion **12**(2): 129-136.
- Liu, Y. and M. M. Sharma (2005). Effect of Fracture Width and Fluid Rheology on Proppant Settling and Retardation: An Experimental Study. SPE Annual Technical Conference and Exhibition. Dallas, Texas, Society of Petroleum Engineers.
- Machado, J. C. V. and A. F. L. Aragao (1990). Gel Strength as Related to Carrying Capacity of Drilling Fluids. SPE Latin America Petroleum Engineering Conference. Rio de Janeiro, Brazil, 1990 Copyright 1990, Society of Petroleum Engineers Inc.
- Mezger, T. G. (2011). The Rheology Handbook. Hanover, European Coating Tech Files.
- Nakajima, M. and N. V. Bot (2002). Silicate/Enhanced Low Shear Rate Viscosity (LSRV) Drilling Fluid System and New Drilling Approach in Rang Dong Field, Society of Petroleum Engineers.
- Novotny, E. J. (1977). PROPPANT TRANSPORT. SPE Annual Fall Technical Conference and Exhibition. Denver, Colorado, 1977 Copyright 1977, American Institute of Mining, Metallurgical, and Petroleum Engineers, Inc.
- Pilehvari, A. A., J. J. Azar and S. A. Shirazi (1999). "State-of-the-Art Cuttings Transport in Horizontal Wellbores." SPE Drilling & Completion **14**(3): 196-200.
- Powell, J. W., C. F. Parks and J. M. Seheult (1991). Xanthan and Welan: The Effects Of Critical Polymer Concentration On Rheology and Fluid Performance. International Arctic

Technology Conference. Anchorage, Alaska, 1991 Copyright 1991, Society of Petroleum Engineers, Inc.

Sample, K. J. and A. T. Bourgoyne (1977). AN EXPERIMENTAL EVALUATION OF CORRELATIONS USED FOR PREDICTING CUTTING SLIP VELOCITY. SPE Annual Fall Technical Conference and Exhibition. Denver, Colorado, 1977 Copyright 1977, American Institute of Mining, Metallurgical, and Petroleum Engineers, Inc.

Sifferman, T. R., G. M. Myers, E. L. Haden and H. A. Wahl (1974). "Drill Cutting Transport in Full Scale Vertical Annuli." Journal of Petroleum Technology **26**(11): 1295-1302.

University of Tennessee, D. o. p. (2008). Studio Session 9.

Walker, R. E. and T. M. Mayes (1975). "Design of Muds for Carrying Capacity." Journal of Petroleum Technology **27**(7): 893-900.

Wolfram Company (2013).

Appendix A. Experimental device and particles



Figure 24. Experimental device used for investigation of particle slip velocity under steady state laminar flow

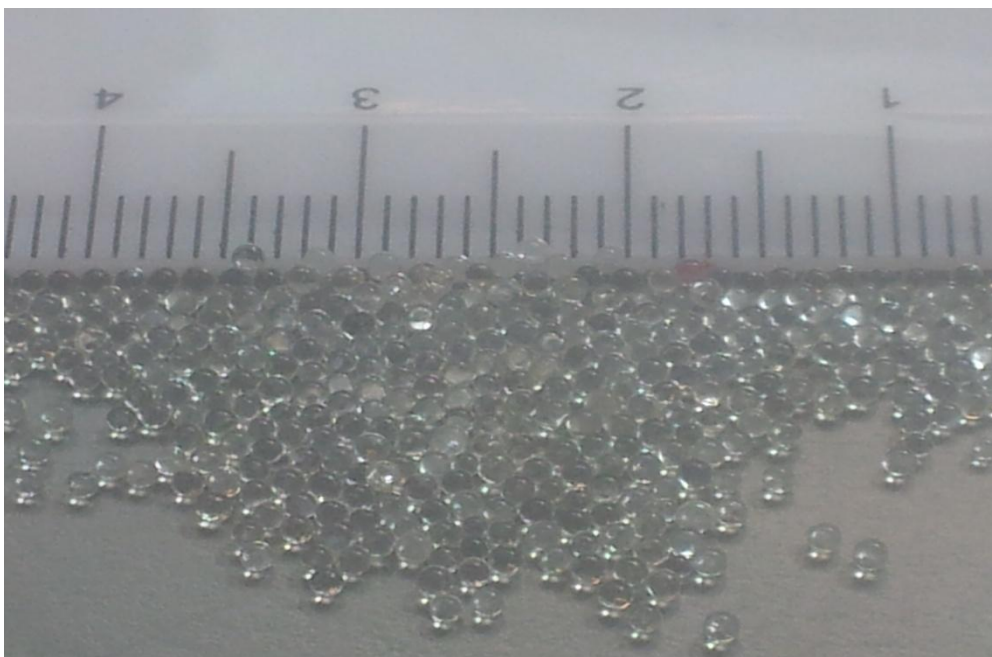


Figure 25. Non-spherical particle used during experimental investigation ($d=3.387\text{mm}$)

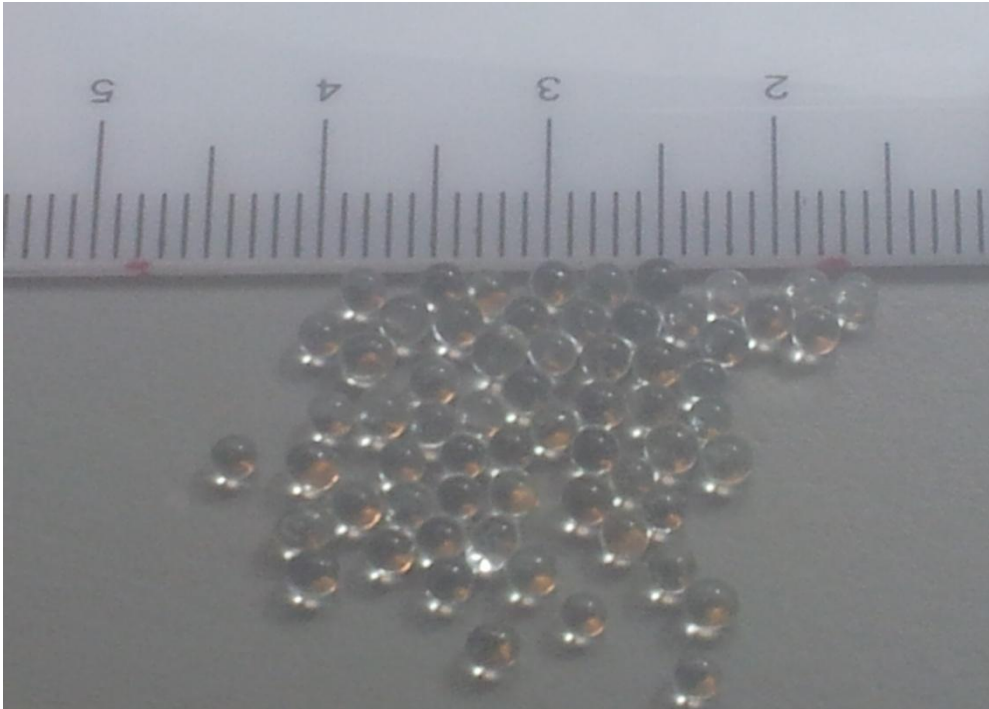


Figure 26. Spherical particle used during experimental investigation ($d=2\text{mm}$)



Figure 27. Non-spherical particle used during experimental investigation ($d=3.387\text{mm}$)

Appendix B. Rheological properties of all three fluids samples used during measuring of slip velocities

Table 2. Rheological properties of 5% PHPA polymer-water mixture.

Revoluti on	Shear rate	Dial Readings	S	Viscosi ty	Shear stress	Shear stress	n	K	Densi ty	10 seconds	1 minut e	10 minutes
RPM	1/s	-	-	cP	lb/ft ²	Pa	-	Pa s	kg/m ³	Θ	Θ	Θ
600	1022	63	0.5	31.5	67	32.0	0.44	1.54	1001	5.5	5.5	6
300	511	46.5	1	46.5	49	23.6						
200	341	39	1.5	58.5	41	19.8						
100	170	29	3	87	31	14.7						
6	10	8	50	400	8	4.1						
3	5	6	100	600	6	3.0						

Table 3. Rheological properties of 10% PHPA polymer-water mixture

Revoluti on	Shear rate	Dial Readings	S	Viscosi ty	Shear stress	Shear stress	n	K	Densi ty	10 seconds	1 minut e	10 minutes
RPM	1/s	-	-	cP	lb/ft ²	Pa	-	Pa s	kg/m ³	Θ	Θ	Θ
600	1022	97.5	0.5	48.8	103	49	0.478	1.88	1001	3.5	4	4
300	511	70	1	70	74	36						
200	341	57	1.5	85.5	60	29						
100	170	38.5	3	115.5	41	20						
6	10	6	50	300	6	3						
3	5	4	100	400	4	2						

Table 4. Rheological properties of 20% PHPA polymer-water mixture

Revoluti on	Shear rate	Dial Readings	S	Viscosi ty	Shear stress	Shear stress	n	K	Densi ty	10 seconds	1 minut e	10 minutes
RPM	1/s	-	-	cP	lb/ft ²	Pa	-	Pa s	kg/m ³	Θ	Θ	Θ
600	1022	245.5	0.5	122.75	260.23	124.598	0.2921	16.5	1003	46	47	47
300	511	200.5	1	200.5	212.53	101.759						
200	340	177	1.5	265.5	187.62	89.8325						
100	170	143.5	3	430.5	152.11	72.8303						
6	10	60	50	3000	63.6	30.4517						
3	5	46	100	4600	48.76	23.3463						

Appendix C. Calculated (theoretical) results of stagnant condition

Table 5. Experimental data (and input data (blue) and theoretically calculated results (red) based on shear rates of v/d for fluid sample 5%

	D cylinder	Particle size	Velocity (practical)	Eff. Viscosity	Density	Density (fluid)	Gravity	Velocity (theory)	Velocity (practical)	Particle-to-tube D	Wall Factor	Velocity (Wall factor)	Error	Drag	Reynolds
	m	m	m/s	Pa	kg/m ³	kg/m ³	m/s ²	m/s	m/s				%		
Glass	39.58	0.0003	0.000083	3.16	2600	1001	9.8	0.000025	0.00008	0.00008	1.0000	0.00008	70	10194932	0.00002
	39.58	0.001	0.001	1.54	2600	1001	9.8	0.00057	0.00100	0.00025	0.99995	0.001	43	64960	0.000369
	39.58	0.002	0.004	1.04	2600	1001	9.8	0.0033	0.00400	0.00051	0.9999	0.004	16	3726	0.006441
Non-sphere	39.58	0.003387	0.011	0.792	2672	1001	9.8	0.0132	0.01100	0.00086	0.99982	0.011	20	426	0.056368

Table 6. Experimental data (and input data (blue) and theoretically calculated results (red) based on shear rates of $3*v/d$ for fluid sample 5%

	D cylinder	Particle size	Velocity (practical)	Eff. Viscosity	Density	Density (fluid)	Gravity	Velocity (theory)	Velocity (practical)	Particle-to-tube D	Wall Factor	Velocity (Wall factor)	Error	Drag	Reynolds
	m	m	m/s	Pa	kg/m ³	kg/m ³	m/s ²	m/s	m/s				%		
Glass	39.58	0.0003	0.000083	1.71	2600	1001	9.8	0.00005	0.000083	0.00001	1	0.0001	45	2966304	0.00008
	39.58	0.001	0.001	0.83	2600	1001	9.8	0.0011	0.001	0.00003	1	0.001	5	18901	0.0013
	39.58	0.002	0.004	0.56	2600	1001	9.8	0.006	0.004	0.00005	1	0.004	55	1084	0.0221
Non-sphere	39.58	0.00339	0.011	0.43	2672	1001	9.8	0.02	0.011	0.00009	1	0.01	122	124	0.19

Table 7. Experimental data (and input data (blue) and theoretically calculated results (red) based on shear rates of v/d for fluid sample 10%

	D cylinder	Particle size	Velocity	Eff. Viscosity	Density	Density (fluid)	Gravity	Velocity (theory)	Velocity (practical)	Particle-to-tube D	Wall Factor	Velocity (Wall factor)	Error	Drag	Reynolds
	m	m	m/s	Pa	kg/m ³	kg/m ³	m/s ²	m/s	m/s				%		
Glass	39.58	0.0003	0.0004	1.55	2600	1002	9.8	0.00005	0.0004	0.00001	1	0.0004	87	2453104	0.00001
	39.58	0.001	0.003	1.02	2600	1002	9.8	0.0009	0.003	0.00003	1	0.003	71	28408	0.0008
	39.58	0.002	0.012	0.71	2600	1002	9.8	0.005	0.012	0.00005	1	0.012	59	1722	0.014
Non-sphere	39.58	0.003	0.023	0.66	2672	1002	9.8	0.016	0.023	0.00009	1	0.02	32	298	0.08

Table 8. Experimental data (and input data (blue) and theoretically calculated results (red) based on shear rates of v/d for fluid sample 20%

	D cylinder	Particle size	Velocity	Eff. Viscosity	Density	Density (fluid)	Gravity	Velocity (theory)	Velocity (practical)	Particle-to- tube D	Wall Factor	Velocity (Wall factor)	Err or	Drag	Reynold s
	m	mm	m/s	Pa	kg/ m ³	kg/m ³	m/s ²	m/s	m/s				%		
Gla ss	39.58	0.0003			260 0	1003	9.8			0.00001	1				
	39.58	0.001	0.00 003	196.97 11	260 0	1003	9.8	0.000004	0.00003	0.00003	1	0.00003	85	106771 8846	0.0000 0002
	39.58	0.002	0.00 011	128.25 06	260 0	1003	9.8	0.00003	0.00011	0.00005	1	0.0001	75	565823 06	0.0000 004
Non - sph ere	39.58	0.0034	0.00 022	114.00 37	267 2	1003	9.8	0.0001	0.00022	0.00009	1	0.00022	58	880830 7	0.0000 03

Appendix D. Calculated (theoretical) results of dynamic condition

Table 9. Input data (blue) and theoretically computed result for steady state laminar flow in sample 5%

	Particle size	Particle Velocity	Eff. Viscosity	Density	Density (fluid)	Gravit y	Velocity (theory)	Drag	Reynolds
	m	m/s	Pa	kg/m3	kg/m3	m/s2	m/s		
Glas s	0.001	0.0007	1.25	2600	1001	9.8	0.0007	4307 6	0.00056
	0.001	0.0007	1.26	2600	1001	9.8	0.0007	4363 7	0.0005
	0.002	0.0022	1.61	2600	1001	9.8	0.002	8954	0.0027
	0.002	0.0171	5.14	7850	1001	9.8	0.003	2119 8	0.0011
	0.001	0.0018	2.14	7850	1001	9.8	0.002	2944 3	0.0008
	0.002	0.0017	1.42	2672	1001	9.8	0.003	6648	0.0036

Table 10. Input data (blue) and theoretically computed results for steady state laminar flow in sample 5%

	Height	Volume	Flow time	Flow rate	Area	Mud Velocity	Flow Shear Rate	Velocity (practical)	Error
	M	m3	s	m3/s	m2	m/s	1/s	m/s	%
Glass	0.05	0.0003	755	0.0000003	0.023	0.00001	0.00155	0.0007	0
	0.1	0.0005	135	0.000004	0.035	0.00011	0.01111	0.0007	1
	0.001	0.000003	15	0.0000002	0.01	0.00002	0.00229	0.0022	1
	0.1	0.000502	135	0.0000037	0.035	0.00011	0.01110	0.017	83
	0.05	0.0003	64	0.000004	0.023	0.000174	0.01822	0.0018	3
	0.01	0.0001	11	0.0000046	0.013	0.0004	0.038	0.0017	47

Appendix E. Experimental results of slip velocities in a stagnant fluid

Table 11. Experimental results of slip velocities with respect to particle sizes and tube diameters conducted in standard rheology (water)

Cylinder diameter	Glass ball (mm)		Non-spherical (mm)
	1	2	3.387
mm	m/s	m/s	m/s
39.58	0.18	0.29	0.18
49.37	0.183206	0.289157	0.19
60.2	0.179104	0.296296	0.21
75	0.188976	0.282353	0.21

Table 12. Experimental results of slip velocities with respect to particle size and tube diameters conducted in sample 5%

Cylinder diameter	Glass ball (mm)			Non-spherical (mm)
	0.3	1	2	3.387
mm	m/s	m/s	m/s	m/s
39.58	0.000083	0.00112	0.004	0.011
49.37		0.00098	0.004	0.005
60.2		0.00105	0.004	0.007
75		0.001091	0.004211	0.0075

Table 13. Experimental results of slip velocities with respect to particle size and tube diameters conducted in sample 10%

Cylinder diameter	Glass ball (mm)			Non-spherical (mm)
	0.3	1	2	3.387
mm	m/s	m/s	m/s	m/s
39.58	0.0004	0.003	0.011	0.023
49.37		0.00338	0.014118	0.022
60.2		0.003	0.01	0.02
75		0.003288	0.012	0.02

Table 14. Experimental results of slip velocities with respect to particle size and tube diameters conducted in sample 20%

Cylinder diameter	Glass ball (mm)			Non-spherical (mm)
	0.3	1	2	3.387
mm	m/s	m/s	m/s	m/s
39.58	-	0.00003	0.00011	0.00022
49.37		0.000031	0.00013	0.0002
60.2		0.000032	0.0001	0.00025
75		0.000033	0.00011	0.00024

Table 15. Experimental results of 1mm particle slip velocities with respect to the travel distance in fluid sample 5%

Length	Time	Velocity
m	s	m/s
0.15	127	0.00118
0.2	173	0.00116
0.24	205	0.00117
0.28	244	0.00115

Table 16. Experimental results of 2 mm particle slip velocities with respect to the travel distance in fluid sample 5%

Length	Time	Velocity
m	s	m/s
0.15	33	0.004534
0.2	45	0.004444
0.24	53	0.004528
0.28	65	0.004308

Appendix F. Rheological properties of sample 10% used for the detection of root causes of unexpected behavior (mixing time/solubility of polymer)

Table 17. Rheological properties of the sample 10% measured after 40 seconds of mixing

Revolution	Rotation	Dial Readings	S	Viscosity	Shear stress	Shear stress	n	K
RPM	RPM	-	-	cP	lb/ft ²	Pa	-	Pas
600	1022	42	0.5	21	44.5	21.3	0.869	0.03
300	511	23	1	23	24.4	11.7		
200	341	20	1.5	30	21.2	10.2		
100	170	13	3	39	13.8	6.6		
6	10	5	50	250	5.3	2.5		
3	5	3	100	300	3.2	1.5		

Table 18. Rheological properties of the sample 10% measured after 65 seconds of mixing

Revolution	Rotation	Dial Readings	S	Viscosity	Shear stress	Shear stress	n	K
RPM	RPM	-	-	cP	lb/ft ²	Pa	-	Pas
600	1022	75	0.5	37.5	79.5	38.1	0.346	2.9
300	511	59	1	59	62.5	29.9		
200	341	49	1.5	73.5	51.9	24.9		
100	170	39	3	117	41.3	19.8		
6	10	14	50	700	14.8	7.1		
3	5	12	100	1200	12.7	6.1		

Table 19. Rheological properties of the sample 10% measured after 150 seconds of mixing

Revolution	Rotation	Dial Readings	S	Viscosity	Shear stress	Shear stress	n	K
RPM	RPM	-	-	cP	lb/ft ²	Pa	-	Pas
600	1022	88	0.5	44	93.3	44.7	0.437	1.7
300	511	65	1	65	68.9	33.0		
200	341	54	1.5	81	57.2	27.4		
100	170	43	3	129	45.6	21.8		
6	10	14	50	700	14.8	7.1		
3	5	13	100	1300	13.8	6.6		

Table 20. Rheological properties of the sample 10% measured after 170 seconds of mixing

Revolution	Rotation	Dial Readings	S	Viscosity	Shear stress	Shear stress	n	K
RPM	RPM	-	-	cP	lb/ft ²	Pa	-	Pas
600	1022	108	0.5	54	114.5	54.8	0.329	4.7
300	511	86	1	86	91.2	43.6		
200	341	72	1.5	108	76.3	36.5		
100	170	53	3	159	56.2	26.9		
6	10	19	50	950	20.1	9.6		
3	5	17	100	1700	18.0	8.6		

Appendix G. Rheological properties of sample 10% used for the detection of root cause of unexpected behavior (no action time/ waiting time)

Table 21. Rheological properties of the sample 10% measured immediately right after the mixing in blender

Revolution	Shear rate	Dial Readings	S	Viscosity	Shear stress	Shear stress	n	K	Density
RPM	1/s	-	-	cP	lb/ft ²	Pa	-	Pas	kg/m ³
600	1022	75	0.5	37.5	79.5	38.1	0.346	2.9	1002
300	511	59	1	59	62.5	29.9			
200	341	49	1.5	73.5	51.9	24.9			
100	170	39	3	117	41.3	19.8			
6	10	14	50	700	14.8	7.1			
3	5	12	100	1200	12.7	6.1			

Table 22. Rheological properties of the sample 10% measured after one day since mixed in blender

Revolution	Shear rate	Dial Readings	S	Viscosity	Shear stress	Shear stress	n	K	Density
RPM	1/s	-	-	cP	lb/ft ²	Pa	-	Pas	kg/m ³
600	1022	110	0.5	55	116.6	55.8	0.322	5.1	1002
300	511	88	1	88	93.3	44.7			
200	341	73	1.5	109.5	77.4	37.0			
100	170	55	3	165	58.3	27.9			
6	10	18	50	900	19.1	9.1			
3	5	14	100	1400	14.8	7.1			

Table 23. Rheological properties of the sample 10% measured after three days since mixed in blender

Revolution	Shear rate	Dial Readings	S	Viscosity	Shear stress	Shear stress	n	K	Density
RPM	1/s	-	-	cP	lb/ft ²	Pa	-	Pas	kg/m ³
600	1022	117	0.5	58.5	124.0	59.4	0.363	4.0	1002
300	511	91	1	91	96.5	46.2			
200	341	77	1.5	115.5	81.6	39.1			
100	170	59	3	177	62.5	29.9			
6	10	18	50	900	19.1	9.1			
3	5	14	100	1400	14.8	7.1			

Appendix H. Rheological properties of sample 10% used for the detection of root cause of unexpected behavior (shaking factor)

Table 24. Rheological properties of 10% PHPA polymer-water mixture after 15 seconds of shaking

Revolution	Shear rate	Dial Readings	S	Viscosity	Shear stress	Shear stress	n	K	Density
RPM	1/s	-	-	cP	lb/ft ²	Pa	-	Pas	kg/m ³
600	1022	125	0.5	62.5	132.5	63.4	0.396	3.3	1002
300	511	95	1	95	100.7	48.2			
200	341	81	1.5	121.5	85.9	41.1			
100	170	62	3	186	65.7	31.5			
6	10	20	50	1000	21.2	10.2			
3	5	13	100	1300	13.8	6.6			

Table 25. Rheological properties of 10% PHPA polymer-water mixture after 30 seconds of

Revolution	Shear rate	Dial Readings	S	Viscosity	Shear stress	Shear stress	n	K	Density
RPM	1/s	-	-	cP	lb/ft ²	Pa	-	Pas	kg/m ³
600	1022	126	0.5	63	133.6	63.9	0.392	3.4	1002
300	511	96	1	96	101.8	48.7			
200	341	82	1.5	123	86.9	41.6			
100	170	63	3	189	66.8	32.0			
6	10	21	50	1050	22.3	10.7			
3	5	14	100	1400	14.8	7.1			

Table 26. Rheological properties of 10% PHPA polymer-water mixture after 60 seconds of shaking

Revolution	Shear rate	Dial Readings	S	Viscosity	Shear stress	Shear stress	n	K	Density
RPM	1/s	-	-	cP	lb/ft ²	Pa	-	Pas	kg/m ³
600	1022	127	0.5	63.5	134.6	64.5	0.389	3.5	1002
300	511	97	1	97	102.8	49.2			
200	341	82	1.5	123	86.9	41.6			
100	170	63	3	189	66.8	32.0			
6	10	21	50	1050	22.3	10.7			
3	5	15	100	1500	15.9	7.6			

Appendix I. Drag coefficient and particle Reynolds number exported from the figure 8

Table 27. Data acquired from Applied Drilling Engineering(A.T. Bourgoyne Jr, K.K. Millheim et al. 1986) presented in figure 8 that shows correlation between Drag coefficient (friction factor) and particle Reynolds number.

Particle Reynolds number	Drag coefficient
1	35
0.8	40
0.6	45
0.4	60
0.2	150
0.1	300
0.08	350
0.06	450
0.04	700
0.02	1400
0.01	3000
0.008	3500
0.006	4000
0.004	6000
0.002	12000
0.001	20000

Appendix J. Simple calculation used during experimental investigation

$$1. \rho_p = \frac{0.001}{0.000000374} = 2672 \text{ kg/m}^3$$

$$2. d_{ESD} = \frac{3.69 + 3.27 + 3.2}{3} = 3.387 \text{ mm}$$

$$3. \psi = \frac{\pi^{\frac{1}{3}}(6 * 0.000000374)}{3.69 * 3.27} * 10^6 = 20.8 - \text{ calculation is wrong, since } \psi \leq 1. \text{ Use sphericity provided from the } \mathbf{chapter\ 3.2\ (c)\ section\ sphericity.}$$

$$4. v_s = \frac{0.24}{215} = 0.00112$$

$$5. q_f = \frac{0.0003}{755} = 0.0000003 \text{ m}^3 / s$$